Annotations from knopHSTpostsub5saul.pdf

Page 31

Annotation 1; Label: Comment; Date: 7/14/2003 12:01:45 AM

Annotation 2; Label: Comment; Date: 7/14/2003 12:01:54 AM

Annotation 3; Label: Comment; Date: 7/14/2003 12:02:05 AM

Annotation 4; Label: Comment; Date: 7/14/2003 12:02:21 AM
(

Page 32

Annotation 1; Label: Comment; Date: 7/14/2003 12:03:04 AM

Annotation 2; Label: Comment; Date: 7/14/2003 12:03:21 AM
(P99)

Page 34

Annotation 1; Label: Comment; Date: 7/14/2003 12:04:21 AM

Annotation 2; Label: Comment; Date: 7/14/2003 12:04:30 AM

Annotation 3; Label: Comment; Date: 7/14/2003 12:04:45 AM
systematic

Annotation 4; Label: Comment; Date: 7/14/2003 12:04:47 AM
0.13.

Annotation 5; Label: Comment; Date: 7/14/2003 12:05:01 AM
statistical

Annotation 6; Label: Comment; Date: 7/14/2003 12:05:26 AM
0.15

Annotation 7; Label: Comment; Date: 7/14/2003 12:06:05 AM
[[[These corrections are what was meant here?]]]

Page 35

Annotation 1; Label: Comment; Date: 7/14/2003 12:06:30 AM

Annotation 2; Label: Comment; Date: 7/14/2003 12:06:37 AM
they are most uncertain,

Annotation 3; Label: Comment; Date: 7/14/2003 12:07:11 AM
the statistical uncertainty is largest

Page 36

Annotation 1; Label: Comment; Date: 7/14/2003 12:08:07 AM

Annotation 2; Label: Comment; Date: 7/14/2003 12:08:12 AM
crudest

Annotation 3; Label: Comment; Date: 7/14/2003 12:08:22 AM
most general

Annotation 4; Label: Comment; Date: 7/14/2003 12:09:01 AM
[[[Do you think "most general" is better than "most basic"?]]]

Page 37

Annotation 1; Label: Comment; Date: 7/14/2003 12:13:20 AM

Annotation 2; Label: Comment; Date: 7/14/2003 12:13:24 AM

Annotation 3; Label: Comment; Date: 7/14/2003 12:13:40 AM
for a given supernova

Annotation 4; Label: Comment; Date: 7/14/2003 12:13:57 AM
for a given supernova

Page 42

Annotation 1; Label: Comment; Date: 7/14/2003 12:15:46 AM

Annotation 2; Label: Comment; Date: 7/14/2003 12:17:01 AM
, astro-ph/0303428

Annotation 3; Label: Comment; Date: 7/14/2003 12:17:14 AM

Page 49

Annotation 1; Label: Comment; Date: 7/14/2003 12:18:34 AM

Annotation 2; Label: Comment; Date: 7/14/2003 12:18:43 AM
Alternate

Annotation 3; Label: Comment; Date: 7/14/2003 12:19:14 AM
with a linear redshift scale

Annotation 4; Label: Comment; Date: 7/14/2003 12:20:04 AM
[[[I think we should go with most of the caption modifications that Greg made, but with this one addition.]]]

Page 51

Annotation 1; Label: Comment; Date: 7/14/2003 12:20:46 AM
Primary

Annotation 2; Label: Comment; Date: 7/14/2003 12:21:14 AM

Annotation 3; Label: Comment; Date: 7/14/2003 12:21:34 AM
a

Annotation 4; Label: Comment; Date: 7/14/2003 12:22:47 AM
this paper's primary analysis, the

Page 52

Annotation 1; Label: Comment; Date: 7/14/2003 12:23:17 AM

Annotation 2; Label: Comment; Date: 7/14/2003 12:23:24 AM

Annotation 3; Label: Comment; Date: 7/14/2003 12:23:51 AM
[[[Can you get a little more contract between these two shading colors?]]]

Page 53

Annotation 1; Label: Comment; Date: 7/14/2003 12:24:11 AM

Annotation 2; Label: Comment; Date: 7/14/2003 12:24:19 AM
Severely

Annotation 3; Label: Comment; Date: 7/14/2003 12:25:01 AM
significantly

Annotation 4; Label: Comment; Date: 7/14/2003 12:26:01 AM
[[[Also, make the words in this label lower-case, like they are in the following two labels, below.]]]

Annotation 5; Label: Comment; Date: 7/14/2003 12:26:14 AM

Annotation 6; Label: Comment; Date: 7/14/2003 12:26:34 AM

Annotation 7; Label: Comment; Date: 7/14/2003 12:27:35 AM

Annotation 8; Label: Comment; Date: 7/14/2003 12:28:22 AM
[[[Can "as Published" be centered under "Reiss et al. (1998)?]]]

Page 54

Annotation 1; Label: Comment; Date: 7/14/2003 12:29:31 AM

Annotation 2; Label: Comment; Date: 7/14/2003 12:30:54 AM
for Omega_M and Omega_Lambda, combining

Annotation 3; Label: Comment; Date: 7/14/2003 12:30:30 AM
M and

Annotation 4; Label: Comment; Date: 7/14/2003 12:30:58 AM
which combine

Page 56

Annotation 1; Label: Comment; Date: 7/14/2003 12:32:31 AM
our standard t

Annotation 2; Label: Comment; Date: 7/14/2003 12:32:38 AM

Annotation 3; Label: Comment; Date: 7/14/2003 12:33:08 AM
the fit to the full primary subset,

Annotation 4; Label: Comment; Date: 7/14/2003 12:33:28 AM

Page 57

Annotation 1; Label: Comment; Date: 7/14/2003 12:34:27 AM

Annotation 2; Label: Comment; Date: 7/14/2003 12:34:47 AM
and extinction-corrected

Annotation 3; Label: Comment; Date: 7/14/2003 12:35:08 AM
[[[Is this correct? Are these points extinction corrected?]]]

Page 60

Annotation 1; Label: Comment; Date: 7/14/2003 12:36:11 AM

Annotation 2; Label: Comment; Date: 7/14/2003 12:37:43 AM

Annotation 3; Label: Comment; Date: 7/14/2003 12:38:32 AM
since the slope, alpha, of the stretch-luminosity relation is also a fit parameter.

Annotation 4; Label: Comment; Date: 7/14/2003 12:38:37 AM
due to the fact that the stretch/luminosity slope is a t parameter,

Annotation 5; Label: Comment; Date: 7/14/2003 12:43:38 AM
Stretch luminosity corrected effective B-band peak magnitude: {m_B}^{eff} \equiv m_X + \alpha(s -1) - K_{BX} - A_X .

Annotation 6; Label: Comment; Date: 7/14/2003 12:43:43 AM
the value in column b, including the stretch correction

Annotation 7; Label: Comment; Date: 7/14/2003 12:43:50 AM

Annotation 8; Label: Comment; Date: 7/14/2003 12:44:05 AM

Annotation 9; Label: Comment; Date: 7/14/2003 12:46:50 AM
[[[The footnote c would be much better written using an equation (like this one, based on the footnote 9 of Table 1 of P99).   Is this equation correct here?]]]

Page 61

Annotation 1; Label: Comment; Date: 7/14/2003 12:47:54 AM
c: Includes the stretch/luminosity correction and all uncertainties used in ts to the low-extinction subset; see note c in Table 3. d: Includes the stretch/luminosity and host-galaxy extinction corrections, and all uncertainties used in ts d

Annotation 2; Label: Comment; Date: 7/14/2003 12:48:49 AM
[[[It's probably better to just copy the same footnote as in the other tables, here -- just like all the other footnotes -- instead of referring to the other table.]]]

Page 62

Annotation 1; Label: Comment; Date: 7/14/2003 12:50:08 AM
d: Includes the stretch/luminosity and host-galaxy extinction corrections, and all uncertainties used in ts with host-galaxy

Annotation 2; Label: Comment; Date: 7/14/2003 12:50:27 AM
[[Copy full footnote here too.]]]

Annotation 3; Label: Comment; Date: 7/14/2003 12:51:10 AM
a

Annotation 4; Label: Comment; Date: 7/14/2003 12:51:26 AM

Annotation 5; Label: Comment; Date: 7/14/2003 12:51:32 AM

Annotation 6; Label: Comment; Date: 7/14/2003 12:52:26 AM
Footnote superscript "a" should now be moved over here, to column 1, i.e., SN^a

Annotation 7; Label: Comment; Date: 7/14/2003 12:54:46 AM
b: This is the measured peak magnitude of the B-band lightcurve.

Annotation 8; Label: Comment; Date: 7/14/2003 12:55:00 AM
e: This value has been K-corrected and corrected for Galactic extinction. f: This is the measured B-V color at the epoch of rest-frame B-band lightcurve maximum. g: Schlegel, Finkbeiner, & Davis (1998); this extinction is already included in the quoted values of mB in column c. h: These supernovae are excluded from the indicated subsets; x 2.5.

Annotation 9; Label: Comment; Date: 7/14/2003 12:55:43 AM

Annotation 10; Label: Comment; Date: 7/14/2003 12:55:48 AM

Annotation 11; Label: Comment; Date: 7/14/2003 12:57:03 AM
[[[I think almost all of these footnotes (or the superscripts connected to them) are incorrect -- they don't refer to the correct columns.]]]

Annotation 12; Label: Comment; Date: 7/14/2003 12:57:28 AM
mX

Annotation 13; Label: Comment; Date: 7/14/2003 12:57:39 AM

Annotation 14; Label: Comment; Date: 7/14/2003 1:00:26 AM
I think this column should not be m_X, but rather m_B^observed (and then the next column should be m_B with a superscript referring to a footnote that says it is the m_B^observed - K_{BB} where K_{BB} is the B band K correction).

Page 65

Annotation 1; Label: Comment; Date: 7/14/2003 1:01:01 AM

Annotation 2; Label: Comment; Date: 7/14/2003 1:01:07 AM
Errors

Annotation 3; Label: Comment; Date: 7/14/2003 1:01:46 AM
Uncertainties

Annotation 4; Label: Comment; Date: 7/14/2003 1:01:59 AM
the low-extinction subset

Annotation 5; Label: Comment; Date: 7/14/2003 1:02:09 AM
ts (Fit 3)

Annotation 6; Label: Comment; Date: 7/14/2003 1:02:21 AM

Annotation 7; Label: Comment; Date: 7/14/2003 1:02:32 AM

fit

2001; Wang, Holz, & Munshi 2002; Minty, Heavens, & Hawkins 2002; Amanullah, Mörtsell & Goobar 2003; Dalal *et al.* 2003; Oguri, Suto, & Turner 2003), especially in relation to the P99 and Riess *et al.* (1998) SN datasets. A very conservative assumption of an "empty beam" model in a universe filled with compact objects allowed P99 to demonstrate that gravitational lensing does not alter the case for dark energy.

Gravitational lensing may result in a biased determination of the cosmological parameter determination, as discussed in Amanullah, Mörtsell & Goobar (2003). The potential bias increases with the redshift of the supernovae in the sample. For example, for the most distant known Type Ia SN, SN1997ff at z=1.7, there is evidence for significant magnification, $\Delta m \sim$ 0.3 (Lewis & Ibata 2001; Mörtsell, Gunnarsson & Goobar 2001; Benitez *et al.* 2002).

As the SN sample considered in this paper does not reach as far, the (de)magnification distortions are expected to be small, in general below 0.05 magnitudes, and less than 1% for the cases considered in P99. To estimate the systematic uncertainties in the cosmological parameters we have used the SNOC package (Goobar *et al.* 2001) to simulate 100 realizations of our data sets assuming a 20% universal fraction of Ω_M in compact objects, i.e. of the same order as the halo fraction deduced for the Milky Way from microlensing along the line of sight to the Large Magellanic Cloud (Alcock *et al.* 2000). The light beams are otherwise assumed to travel through space randomly filled with galaxy halos with mass density equally divided into SIS and NFW profiles, as described in ~~(~~Bergström *et al.* (2000). According to our simulations we find that (for a flat universe) the fitted value of Ω_M is systematically shifted by 0.01 on the average, with a statistical dispersion $\sigma_{\Delta\Omega_{\mathrm{M}}} = 0.01$. We adopt 0.01 as our gravitational lensing systematic error in the flat-universe value of Ω_{M}. The effect on $\Omega_{\mathrm{M}} + \Omega_\Lambda$ is very small compared to other systematics, biasing the sum by only 0.04.

The simulated offsets due to gravitational lensing, when combined with CMB and galaxy redshift distortion measurements, increase the value of w by 0.05; we adopt this as a gravitational lensing systematic on w.

5.7. Supernova Population Drift

In P99 we discussed in detail whether the high-redshift SNe Ia could have systematically different properties than low-redshift SNe Ia, and in particular, whether intrinsic differences might remain after correction for stretch. One might imagine this to occur if the range of the physical parameters controlling SN Ia brightnesses have little overlap between low- and high-redshift such that corrections applied to low-redshift are inappropriate or incomplete for high-redshift SNe Ia. Since P99, considerable additional work has been done to address this issue.

In addition to comparisons of stretch range (P99), as well as spectral (Perlmutter *et al.* 1998; Coil *et al.* 2000) and lightcurve (Goldhaber *et al.* 2001) features, several tests performed directly with the P99 high-redshift SNe Ia have shown excellent consistency with low-redshift SNe Ia. Most recently, in Sullivan *et al.* (2003) we have presented results on the Hubble diagram of distant Type Ia supernovae from P99 that have been morphologically-typed with HST. We found no difference in the cosmological results from their morphologically-segregated subsamples. In particular, E/S0 galaxies—for which one expects the tightest possible correlation between progenitor mass and redshift—not only agree with the cosmological fits using only spiral galaxies, but by themselves confirm the results of P99. This is strong evidence that, while age or metallicity could in principle affect the brightnesses of SNe Ia, stretch correction eliminates these differences. Likewise, the lightcurve rise-time—a possible indicator of the energetics of the SN explosion (see Nugent *et al.* 1995; Hoeflich, Wheeler, & Thielemann 1998)—while initially suggested to be different between high- and low-redshift SNe Ia (Riess *et al.* 1999b), has been demonstrated to agree very well (within 1.8 ± 1.2 days, Aldering, Knop, & Nugent 2000).

On the theoretical side, the SN formation models of Kobayashi *et al.* (1998) and Nomoto, Nakamura, & Kobayashi (1999) suggest that the progenitor binary system must have $[Fe/H] > \ 1$ in order to produce a SN Ia. This would impose a lower limit to the metallicities of all SNe Ia, and thus limit the extent of any metallicity-induced brightness differences between high- and low-redshift SNe Ia. On the empirical side, the lack of a gradient in the intrinsic luminosities of SNe Ia with galactocentric distance, coupled with the fact that metallicity gradients are common in spiral galaxies (Henry & Worthey 1999), lead Ivanov, Hamuy, & Pinto (2000) to suggest that metallicity is not a key parameter in controlling SNe Ia brightnesses at optical wavelengths—though note that Lentz *et al.* (2000) show how it can affect the ultraviolet. In addition, Hamuy *et al.* (2000, 2001) find that lightcurve width is not dependent on host-galaxy metallicity.

Alternatively, population age effects, including pre-explosion cooling undergone by the progenitor white dwarf and other effects linked to the mass of the primary exploding white dwarf have been suggested (for a review, see Ruiz-Lapuente 2003). As the local sample of SNe Ia represents populations of all ages and metallicities, both effects can be studied locally. Several low-redshift studies have presented data suggesting that SNe Ia intrinsic luminosities (i.e., those prior to stretch correction) may correlate with host-galaxy environment (Hamuy *et al.* 1996b; Branch, Romanishin, & Baron 1996; Wang, Hoeflich, & Wheeler 1997; Hamuy *et al.* 2000; Ivanov, Hamuy, & Pinto 2000; Howell 2001; Wang *et al.* 2003, R99). These findings are actually encouraging, since unlike stretch itself, there is some hope that host-galaxy environment variations can be translated into physical parameters such as age and metallicity. These parameters can help relate any drifts in the SNe Ia population to evolution of the host galaxies.

More importantly for cosmology, R99 used their sample of 22 local SNe Ia to demonstrate that any brightness variations between SNe Ia in different host-galaxy environments disappear after correction for lightcurve width. We have quantified this agreement using a larger local sample of supernovae compiled in Wang *et al.* (2003), 14 of which have E/S0 hosts and 27 of which have spiral hosts. We find that after lightcurve-width correction there can be less than a 0.01 ± 0.05 mag offset between SNe Ia in local spirals and ellipticals. This indicates that lightcurve width is able to correct for age or other differences.

Finally, Wang *et al.* (2003) demonstrate a new method, *CMAGIC*, which is able to standardize the vast majority of local SNe Ia to within 0.08 mag (in contrast to ~ 0.11 mag which lightcurve-width corrections can attain (Phillips *et al.* 1999)). This imposes even more severe limits on the fraction of SNe Ia generated by any alternate progenitor scenario, or requires that variations in the progenitor properties have little effect on whether the resulting SN can be standardized.

The data from the new SNe Ia presented here do offer one new test for consistency between low- and high-redshift SNe Ia. The quality of our HST data provides measurements of the SN peak magnitudes and lightcurve widths rivaling those for nearby SNe Ia. This allows a direct comparison between the stretch-luminosity relations at low- and high-redshifts. Figure 14 shows that the HST high-redshift supernovae are found at similar stretches and luminosities as the low-redshift supernovae. The low- and high-redshift samples are consistent with the same stretch-luminosity relationship, although it is primarily the low-redshift supernovae that prefer a non-zero slope for this relationship.

5.8. Possible Additional Sources of Systematic Uncertainties

Other potential sources of systematic uncertainties have been suggested. Aguirre (1999a,b) and Aguirre & Zoltan (2000) argued that the presence of "grey" dust, i.e. a homogeneous intergalactic component with weak differential extinction properties over the rest-frame optical wavelength regime could not be ruled out by the P99 data. Since then, measurements of a SN Ia at $z \simeq 1.7$ (Riess *et al.* 2001) were claimed to rule out the "grey" dust scenario as a non-cosmological alternative explanation to the dimming of high-redshift supernovae; however, there remain some outstanding issues with this interpretation (e.g., Goobar, Bergström, & Mörtsell 2002; Blakeslee *et al.* 2003). A direct test for extinction over a wide wavelength range, rest-frame B-I, have been performed by Riess *et al.* (2000) on a single supernova at $z = 0.46$, SN 1999Q, which showed no grey dust signature; however, see Nobili *et al.* (2003). Although the situation remains inconclusive, there is no direct evidence that "grey" dust is a dominant source of uncertainties. It remains an important issue to be addressed by future data sets including near-infrared observations.

More recently, the possibility of axion-photon oscillations making high-redshift supernovae appear dimmer was suggested by Csaki, Kaloper, & Terning (2002). This attenuation would be wavelength dependent, and thus could be explored with spectroscopic studies of high-shift sources (Mörtsell, Bergstrom, & Goobar 2002). Preliminary studies of QSO spectra between $z = 0.15$ and $z = 5.3$ set a very conservative upper limit on the possible dimming of z∼0.8 supernovae to 0.2 magnitudes (Mörtsell & Goobar 2003)

For the current data sample, the above mentioned sources of systematic uncertainties are difficult to quantify at present, but are believed to be subdominant in the total error budget.

5.9. Total Identified Systematic Uncertainty

The identified systematic errors are summarized in Table 9. Adding together these errors in quadrature, we obtain a total systematic error of 0.04 on the flat-universe value of $\Omega_{\rm M}$ (along approximately the minor axis of the confidence ellipses shown in $\Omega_{\rm M}$ vs. Ω_Λ plots); this is smaller than but approaching our statistical uncertainty of 0.06. The total systematic uncertainty on $\Omega_{\rm M} + \Omega_\Lambda$ is 0.96 (along approximately the major axis of the confidence ellipses). Finally, for the low-extinction subset, we have a systematic uncertainty on constant w of 0.09, less than our high-side ~~systematic~~ statistical uncertainty of ~~0.13.~~ 0.15

[[[These corrections are what was meant here?]]]

For fits with host-galaxy extinction corrections applied, we have to consider the additional systematic effects of an uncertainty in the intrinsic value of U-B on determined color excesses, and of dust properties. In this case, we have a total systematic error of 0.09 on the flat-universe value of $\Omega_{\rm M}$ or Ω_Λ, and a total systematic error of 2.0 on $\Omega_{\rm M} + \Omega_\Lambda$; as discussed in § 5.4, this is likely to be an overestimate of the true systematic error. The total systematic uncertainty on constant w for the extinction-corrected full primary sample is 0.15.

6. Summary and Conclusions

1. We present a new, independent set of eleven high-redshift supernovae ($z = 0.36$–0.86). These supernovae have very high-quality photometry measured with WFPC2 on the

HST. The higher quality lightcurve measurements have small enough errors on each $E(B\text{-}V)$ measurement to allow an unbiased correction of host-galaxy reddening. We have performed improved color and K-corrections, necessary to combine WFPC2 photometric filters with ground-based photometric filters.

2. The cosmological fits to $\Omega_{\rm M}$ and Ω_Λ are consistent with the SCP's previous results (P99), providing strong evidence for a cosmological constant. This is a significant confirmation of the results of P99 and Riess *et al.* (1998), and represents a completely new set of high-redshift supernovae yielding the same results as the earlier supernova work. Moreover, these results are consistent with a number of other cosmological measurements, and together with other current cosmological observations is pointing towards a consensus $\Omega_{\rm M} \sim 0.3$, $\Omega_\Lambda \sim 0.7$ Universe.

3. Most identified systematic errors on $\Omega_{\rm M}$ and Ω_Λ affect the cosmological results primarily by moving them along the direction where the statistical uncertainty is largest ~~they are most uncertain,~~ that is, along the major axis of the confidence ellipses. Systematics are much smaller along the minor (approximately $\Omega_{\rm M} \quad \Omega_\Lambda$) axis of the confidence regions, and may be described by giving the systematic error on $\Omega_{\rm M}$ or Ω_Λ alone in the flat-universe case. Our total identified systematic error for the low-extinction sample analysis is 0.04 on the flat-universe value of $\Omega_{\rm M}$ or Ω_Λ. For fits with host-galaxy extinction corrections, a conservative estimate of the total identified systematic error is 0.09.

   In the more uncertain major axis, our total identified systematic error is 0.96 on $\Omega_{\rm M} + \Omega_\Lambda$ for the low-extinction primary subset, and 2.0 on the extinction-corrected full primary subset. Given the large size of these systematics in this direction, any conclusions drawn from the positions of supernova confidence ellipses along this direction should be approached with caution.

4. Under the assumption of a flat universe with vacuum energy (constant $w = \quad 1$), we find a value of $\Omega_{\rm M} = 0.25^{+0.07}_{\ 0.06}$ (statistical) ± 0.04 (identified systematic), or equivalently, a cosmological constant of $\Omega_\Lambda = 0.75^{+0.06}_{\ 0.07}$ (statistical) ± 0.04 (identified systematic). This result is robust to host-galaxy extinction, and a fit with full, unbiased, individual extinction corrections applied yields a flat-universe cosmological constant of $\Omega_\Lambda = 0.72^{+0.10}_{\ 0.11}$ (statistical) ± 0.09 (identified systematic). Our best confidence regions for $\Omega_{\rm M}$ versus Ω_Λ are shown in Figure 8.

5. When combined with the 2dFGRS galaxy redshift distortion measurement and recent CMB data, we find a value for the dark energy equation of state parameter $w = \quad 1.05^{+0.15}_{\ 0.20}$ marginalizing over $\Omega_{\rm M}$ (or a mass density$\Omega_{\rm M} = 0.27^{+0.06}_{\ 0.05}$ marginalizing over w), under the assumptions that the Universe is spatially flat and that w is

constant in time. The identified systematic uncertainty on w is 0.09. The current confidence regions on the flat-universe values of Ω_{M} and w are shown in Figure 12. The supernovae data are consistent with a low-mass Universe dominated by vacuum energy ($w =$ 1), but they are also consistent with a wide range of constant or time-varying dark energy models.

In summary, high-redshift supernovae continue to be the best single tool for directly measuring the density of dark energy. This new set of supernovae observed with the HST confirm and strengthen previous supernova evidence for an accelerating universe, and show that those results are robust even when host-galaxy extinction is fully accounted for. High-redshift supernovae, together with other cosmological measurements, are providing a consistent picture of a low-mass, flat universe filled with dark energy. The next task for cosmologists is to better measure the properties of the dark energy, so as to further our understanding of its nature. Combinations of current cosmological techniques have begun to provide measurements of its most general ~~crudest~~ property (specifically, the equation of state parameter when it is assumed to be constant). Future work will refine these measurements, and in particular reduce the systematic uncertainties that will soon limit the current series of supernova studies. As new instruments become available, it will begin to be possible to relax the condition of a constant equation of state parameter, and to question whether the properties of the dark energy have been changing throughout the history of the Universe.

[[[Do you think "most general" is better than "most basic"?]]]

The authors wish to thank our HST program coordinator, Doug Van Orsow and the excellent HST support staff for their help in the planning, scheduling, and execution of the observations presented herein. Support for this work was provided by NASA through grants HST-GO-07336.01-A and HST-GO-08346.01-A from the Space Telescope Science Institute, which is operated by the Association of Universities for Research in Astronomy, Inc., under NASA contract NAS 5-26555. The authors are indebted to Drs. Malcolm Smith and Patrick Hall for trading several crucial hours of observing time at the CTIO 4m, which played a key role in our SN search in March 1998. The authors acknowledge the tremendous help of the night assistants and support staff at the many telescopes from which data for this paper were obtained; we are particularly grateful to the CTIO staff for crucial support during our key search nights, and to Di Harmer and Paul Smith of the WIYN Queue. We thank Gary Bernstein and Tony Tyson for developing and supporting the Big Throughput Camera at the CTIO 4m. This wide-field camera was important in the discovery of most of the high-redshift supernovae presented in this paper, and enabled the high discovery rate needed to guarantee supernovae for follow-up with HST. The authors are grateful to Eric Linder for the use of his growth-parameter solver, and to Ramon Miguel for assistance with gravitational lensing calculations. We also wish to acknowledge NOAO for providing and supporting the astronomical data reduction package IRAF. The authors wish to recognize and acknowledge the very significant cultural role and reverence that the summit of Mauna Kea has always had within the indigenous Hawaiian community. We are most fortunate to have the opportunity to conduct observations from this mountain. This work was supported in part by the Director, Office of Science, Office of High Energy and Nuclear Physics, of the U.S. Department of Energy under Contract No. DE-AC03-76SF000098, by the Center for Particle Astrophysics, an NSF Science and Technology Center operated by the University of California, Berkeley, under Cooperative Agreement No. AST-91-20005. This work was supported in part by a NASA LTSA grant to PEN, GA, SP, and SED, and WMWV was supported in part by a National Science Foundation Graduate Research Fellowship. A. Goobar is a Royal Swedish Academy Research Fellow supported by a grant from the Knut and Alice Wallenberg Foundation.

A. Lightcurve Data

Tabulated below are lightcurve data for the eleven HST supernovae presented in this paper. For each event, there are two lightcurves, one for R-band and one for I-band. All photometry has been color-corrected to the standard Bessel filters as described in § 3, using color corrections which assume the lightcurve parameters in Table 3. These lightcurves, together with a $7'' \times 7''$ thumbnail of the F675W WFPC2 image closest to maximum light, are shown in Figures 1 and 2. Note that there are correlated errors between the data points. For the ground-based data, there is a covariance because for a given supernova the same final reference images were subtracted from all other ground-based points. Similarly, the HST data include a covariance due to a single background model having been used for all points for a given supernova (see § 2.1). In addition to this, the relative photometric zeropoint magnitudes were determined separately for the ground-based and HST photometry; in the former case, standard stars from Landolt (1992) were used to measure magnitudes of secondary standard stars in the supernova field of view. In the latter case, zeropoints from Dolphin (2000) were used. These covariance matrices will be available from the SCP website.[33]

Because uncertainties are flux uncertainties rather than magnitude uncertainties, each lightcurve is presented in arbitrary flux units. For each lightcurve, the zeropoint necessary to convert these to magnitudes is given. The magnitude may be calculated using the standard formula:

$$m = \quad 2.5 \log f \ + \ m_{zp} \tag{A1}$$

[33]http://supernova.lbl.gov/

where m_{zp} is the quoted zeropoint and f is the flux value from the table. (Because we include early-time and late-time lightcurve points when the supernova flux is undetected given our photometry errors, some of the measured fluxes scatter to negative values. Note that it is impossible to formally calculate a magnitude for these points, and also that flux values are the proper way to quote the data as they better reflect the units in which our photometry errors are approximately Gaussian.)

The telescope used for each data point is indicated. BTC = the Big Throughput Camera on the CTIO 4m telescope. CTIO = the prime focus imager on the CTIO 4m telescope. WIYN = the Nasmyth 2k×2k imager on the WIYN 3.5m telescope at Kitt Peak observatory. INT = the WFC (wide-field camera) on the INT 2.5m telescope at La Palma. KECK = the LRIS imager on the Keck 10m telescope. NTT = the SUSI-2 imager on the NTT 3.6m telescope at ESO. CFHT = the CFHT12K multi-chip imager on the 3.6m CFHT telescope on Mauna Kea in Hawaii. Finally, HSTPC indicates data obtained from the Planetary Camera CCD on WFPC2.

REFERENCES

Aguirre, A., 1999a, ApJ, 512, L19

Aguirre, A., 1999b, ApJ, 525, 583

Aguirre, A., & Zoltan, H., 2000, ApJ, 532, 28

Alcock, C. *et al.*, 2000, ApJ, 542, 281

Aldering, G., Knop, R., & Nugent, P., 2000, AJ, 119, 2110

Allen, A. W., Schmidt, R. W., & Fabian, A. C., 2002, MNRAS, 334, L11

Amanullah, R., Mörtsell, E., & Goobar, A, 2003, A&A397, 819

Appenzeller, I., *et al.*, 1998, ESO Messenger, 94, 1

Bahcall, N. A., Ostriker, J. P., Perlmutter, S., & Steinhardt, P. J., 1999, Science, 284, 1481

Bahcall, N. A., *et al.*, 2003, ApJ, 585, 182

Benitez, N., Riess, A., Nugent, P., Dickinson, M., Chornock, R., & Filippenko, A. V., 2002, ApJ, 577, L1

Bergström, L., Goliath, M., Goobar, A., & Mörtsell, E., 2000, A&A, 358, 13

Blakeslee *et al.*, 2003, ApJ, in press; astro-ph/0302402

Branch, D., & van den Bergh, S., 1993, AJ, 105, 2231

Branch, D., Romanishin, W., & Baron, E., 1996, ApJ, 465, 73

Bennett, C. L., *et al.*, 2003, submitted to ApJ, astro-ph/0302207

Bessell, M. S., 1990, PASP, 102, 1181

Cardelli, J. A., Clayton, G. C., & Mathis, J., S., 1989, ApJ, 345, 245

Coil, A. L. 2000, *et al.*, ApJ, 544, L111

Csáki, C., Kaloper, N., & Terning, J., 2002, Phys. Rev. Lett., 88, 61302

Dalal, N., Holz, D. E., Chen, X., & Frieman, J. A. 2003, ApJ, 585, L11

Dolphin, 2000, PASP, 112, 1397

Dolphin, 2003, http://www.stsci.edu/hst/HST_overview/documents/calworkshop/workshop2002/CW2002_Papers/

Efstathiou, G., *et al.*, 2002, MNRAS, 330, L29

Falco, E. E., *et al.*, 1999, ApJ, 523, 617

Frieman, J. A., Comments Astrophys., 18, 323

Fruchter, A., 2000, private communication

Garnavich, P. M., *et al.*, 1998a, ApJ, 493, L53

Garnavich, P. M., *et al.*, 1998b, ApJ, 509, 74

Goldhaber G., *et al.*, 2001, ApJ, 558, 359

Goobar, A., Mörtsell, E., Amanullah, R., Goliath, M., Bergström, L., & Dahlén, T., 2002, A&A, 392, 757

Goobar, A., Bergström, L., & Mörtsell E., 2002, A&A, 384, 1

Hamuy, M., Phillips, M. M., Maza, J., Wischnjewsky, M., Uomoto, A., Landolt, A. U., & Khatwani, R., 1992, AJ, 102, 208

Hamuy, M., *et al.*, 1996a, AJ, 112, 2408 (H96)

Hamuy, M., Phillips, M. M., Suntzeff, N. B., Schommer, R. A., Maza, J., & Aviles, R., 1996b, AJ, 112, 2391

Hamuy, M., Trager, S. C., Pinto, P. A., Phillips, M. M., Schommer, R. A., Ivanov, V., & Suntzeff, N. B., 2000, AJ, 120, 1479

Hamuy, M., Trager, S. C., Pinto, P. A., Phillips, M. M., Schommer, R. A., Ivanov, V., & Suntzeff, N. B. 2001, AJ, 122, 3506 erratum

Hatano, K., Branch, D., & Deaton, J., 1998, ApJ, 502, 177

Hawkins, E., *et al.*, 2002, submitted to MNRAS, astro-ph/0212375

Henry, R. B. C., & Worthey, G., 1999, PASP, 111, 919

Hoeflich, P., Wheeler, J. C., & Thielmann, F. K., 1998, ApJ, 495, 617

Holz, D. E. 1998, ApJ, 506, L1

Holz, D. E. 2001, ApJ, 556, L71

Holtzman, J. A., Burrows, C. J., Casertano, S., Hester, J. J., Traugher, J. T., Watson, A. M. and Worthey, G., 1995, PASP, 107, 1065

Howell, D. A. 2001, ApJ, 554, L193

Ivanov, V. D., Hamuy, M., & Pinto, P. A., 2000, ApJ, 542, 588

Jaffe, A. H., *et al.*, 2001, Phys. Rev. Lett., 86, 3475

James, F., & Roos, M., 1975, Compt. Phys. Comm. 10, 343

Jha, 2002, PhD thesis, Harvard University

Kantowski, R. 1998, ApJ, 507, 483

Kim, A., Goobar, A., & Perlmutter, S., 1996, PASP, 108, 190

Kim, A., Linder, E., Miquel, & Mostek, 2003, MNRAS, submitted, astro-ph/0304509

Kobayashi, C., Tsujimoto, T., Nomoto, K., Hachisu, I., & Kato, M., 1998, ApJ, 503, L155

Krist, J., & Hook, R., "The Tiny Tim Users Guide", available from STScI

Landolt, A. U., 1992, AJ, 104, 340

Leibundgut B., 2001, ARA&A, 39, 67

Lentz, E. J., Baron, E., Branch, D., Hauschildt, P. H., & Nugent, P. E., 2000, ApJ, 530, 966

Lewis, G. F., & Ibata, R. A., 2001, MNRAS, 324, L25

Li, W., Filippenko, A. V., & Riess, A. G. 2001, ApJ, 546, 719

Linder, E. V. & Jenkins, A., 2003, submitted to MNRAS, astro-ph/0305286

Lira, P., *et al.*, 1998, AJ, 115, 234

Malmquist, K. G., 1924, Medd. Lund Astron. Obs. Ser. II, 32, 64

Malmquist, K. G., 1936, Stockholm Observatory Medd., no. 26

Metcalf, R. B. & Silk, J. 1999, ApJ, 519, L1

Metcalf, R. B. 1999, MNRAS, 305, 746

Minty, E. M., Heavens, A. F., & Hawkins, M. R. S. 2002, MNRAS, 330, 378

Mörtsell, E., Gunnarsson, C., & Goobar, A., 2001, ApJ, 561, 106

Mörtsell, E., Bergström, L., & Goobar, A., 2002, Phys. Rev. D, 66, 047702

Mörtsell, E., & Goobar, A., 2003, Journal of Cosmology and Astroparticle Physics, 04, 003

Nobili, S., Goobar, A., Knop, R., & Nugent, P., 2003, A&A, 404, 901

Nomoto, K., Nakamura, T., & Kobayashi, C. 1999, Ap&SS, 265, 37

Nugent, P., Phillips, M., Baron, E., Branch, D., & Hauschildt, P., 1995, ApJ, 455, L147

Nugent P., Kim, A., & Perlmutter, S., 2002, PASP, 114, 803

O'Donnell, J. E., 1994, ApJ, 422, 158

Oguri, M., Suto, Y., & Turner, E. L. 2003, ApJ, 583, 584

Oke, J. B., *et al.*, 1995, PASP, 107, 375

Perlmutter, S., *et al.*, 1995, ApJ, 440, L41

Perlmutter, S., *et al.*, 1997, ApJ, 483, 565

Perlmutter *et al.*, 1998, Nature, 391, 51

Perlmutter *et al.*, 1999, ApJ, 517, 586 (P99)

Perlmutter S. & Schmidt B., 2003, in "Supernovae & Gamma Ray Bursts", ed. Weiler, K. (Springer) , astro-ph/0303428

Phillips, M. M., 1993, ApJ, 413, L105

Phillips, M. M., Lira, P., Suntzeff, N. B., Schommer, R., A., Hamuy, M., & Maza, J., 1999, AJ, 118, 1766

Pskovski, 1969, Sov. Astr., 12, 750

Richmond *et al.*, 1995, AJ, 109, 2121

Riess, A. G., *et al.*, 1998, AJ, 116, 1009

Riess, A. G., *et al.*, 1999, AJ, 117, 707 (R99)

Riess, A. G., Filippenko, A. V., Li, W., & Schmidt, B. P. 1999, AJ, 118, 2668

Riess, A. G., *et al.*, 2000, ApJ, 536, 62

Riess, A. G., *et al.*, 2001, ApJ, 560, 49

Rowan-Robinson, M., 2002, MNRAS, 332, 352

Ruiz-Lapuente, P., 2003, in "3K, SNs, Clusters: Hunting the Cosmological Parameters", ed. Barbosa et al. (Kluwer Acad. Publ.); astro-ph/0304108

Schlegel, D. J., Finkbeiner, D. P., & Davis, M., 1998, ApJ, 500, 525

Schmidt, B. P., *et al.*, 1998, ApJ, 507, 46

Seljak, U. & Holz, D. E. 1999, A&A, 351, L10

Spergel, *et al.*, 2003, submitted to ApJ, astro-ph/0302209

Sullivan, M., *et al.*, 2003, MNRAS, 340, 1057

Suntzeff, N. B., *et al.*, 1999, AJ, 117, 1175

Tonry, J., *et al.*, 2003, ApJ, in press, astro-ph/0305008

Turner, M., 2001, PASP, 113, 653

Verde, L., *et al.*, 2002, MNRAS, 335, 432

Wambsganss, J., Cen, R., Xu, G., & Ostriker, J. P. 1997, ApJ, 475, L81

Wang, L., Hoeflich, P., & Wheeler, J. C., 1997, ApJ, 483, L29

Wang, Y., Holz, D. E., & Munshi, D. 2002, ApJ, 572, L15

Wang, L., Goldhaber, G., Aldering, G., & Perlmutter, S. 2003, ApJ, in press; astro-ph/0302341

Wells, L. A., *et al.*, 1994, AJ, 108,2233

Whitmore, B., Heyer, I., & Casertano, S., 1999, PASP, 111, 1559

Wu, H., Yan, H. J., & Zou, Z. L., 1995, A&A, 294, L9

This preprint was prepared with the AAS LaTeX macros v5.0.

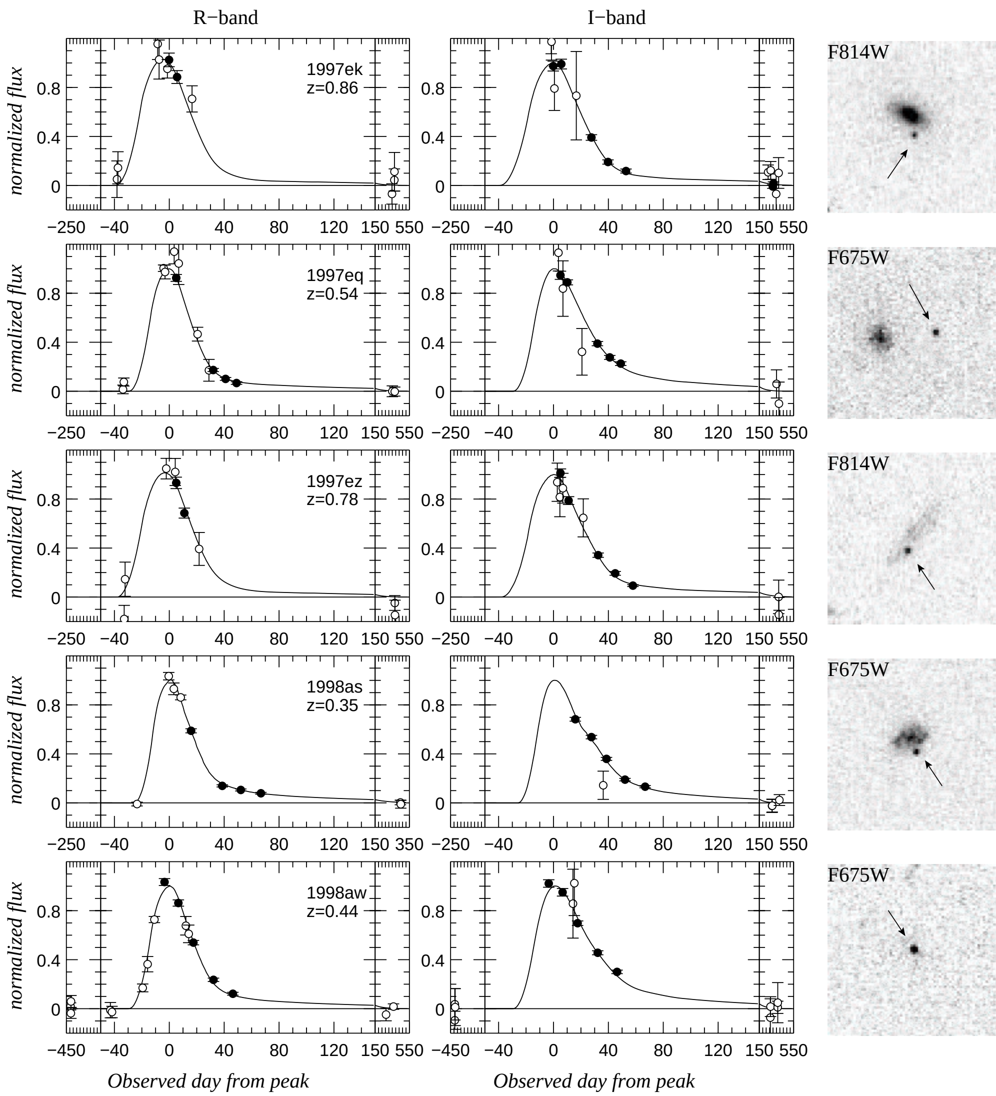

Fig. 1.— Lightcurves and images from the PC CCD on WFPC2 for the HST supernovae reported in this paper. The left column shows the R-band (including F675W HST data), and the middle column shows I-band lightcurves (including F814W HST data). Open circles represent ground-based data points, and filled circles represent WFPC2 data points. Note that there are correlated errors between all of the ground-based points for each supernova in these figures, as a single ground-based zeropoint was used to scale each of them together with the HST photometry. The right column shows $6'' \times 6''$ images, summed from all HST images of the supernova in the indicated filter.

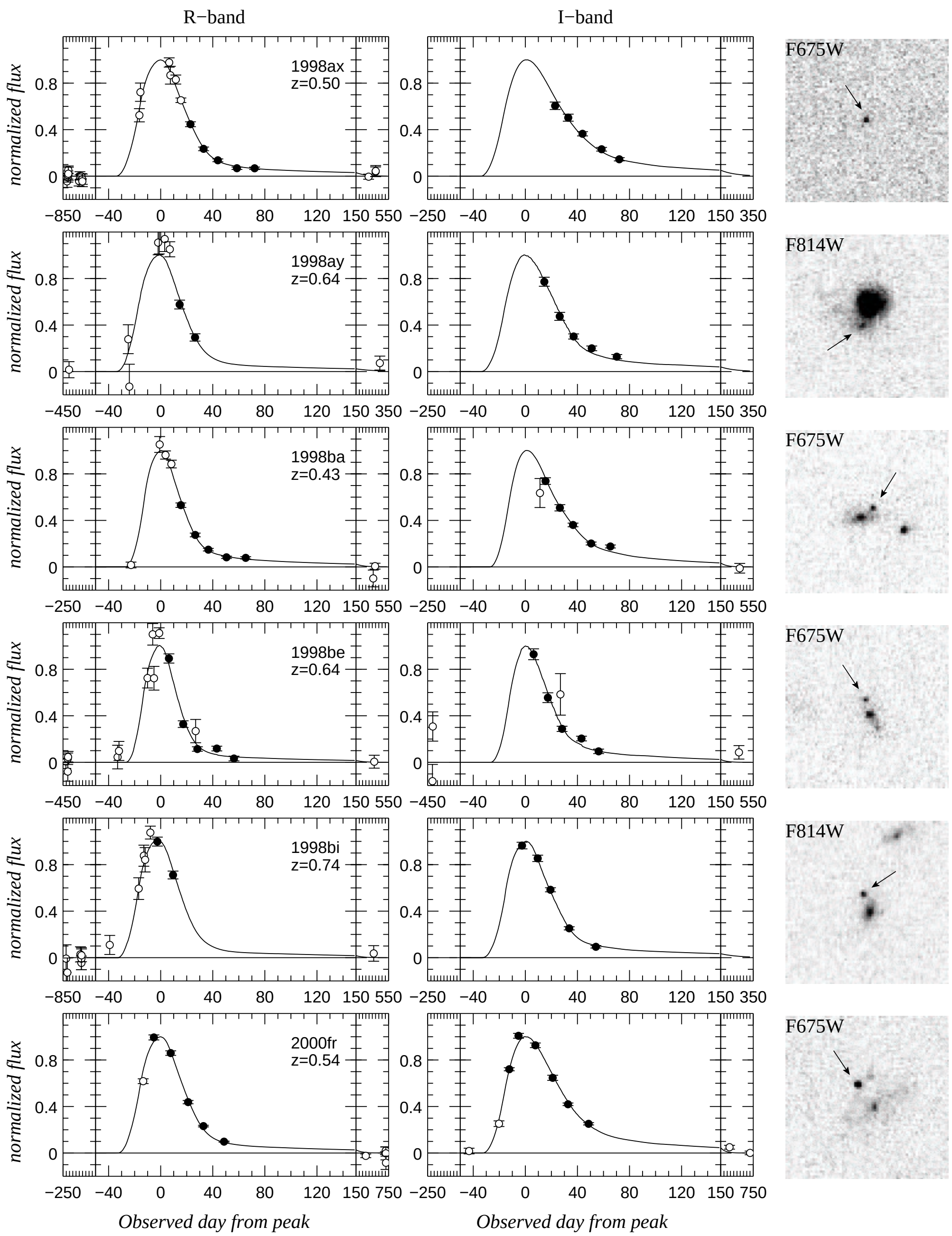

Fig. 2.— Lightcurves and images from the PC CCD on WFPC2 for the HST supernovae reported in this paper (continued). The left column shows the R-band (including F675W HST data), and the middle column shows I-band lightcurves (including F814W HST data). Open circles represent ground-based data points, and filled circles represent WFPC2 data points. Note that there are correlated errors between all of the ground-based points for each supernova in these figures, as a single ground-based zeropoint was used to scale each of them together with the HST photometry. The right column shows $6'' \times 6''$ images, summed from all HST images of the supernova in the indicated filter.

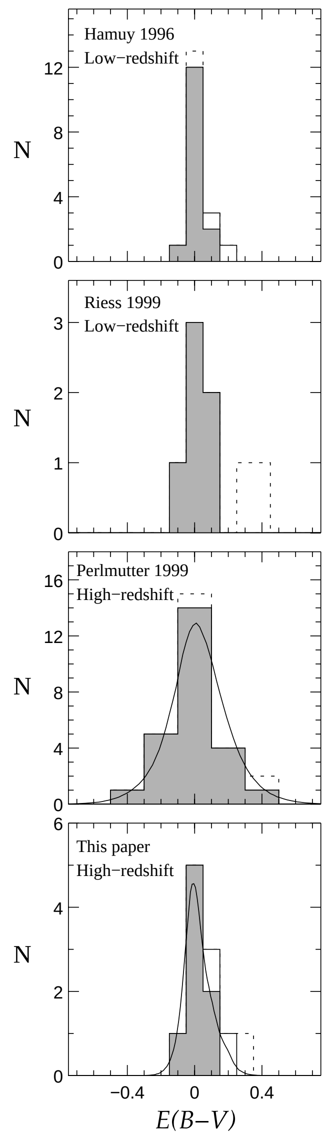

Fig. 3.— Histograms of $E(B\text{-}V)$ for the four samples of supernovae used in this paper. The filled grey histogram represents just the low-extinction subset (Subset 2). The open boxes on top of that represent supernovae which are in the primary subset (Subset 1) but excluded from the low-extinction subset. Finally, the dotted histogram represents those supernovae which are in the full sample but omitted from the primary subset. The solid lines drawn over the bottom two panels is a simulation of the distribution expected if the low-extinction subset of the H96 sample represented the true distribution of SN colors, given the error bars of the low-extinction subset of each high-redshift sample.

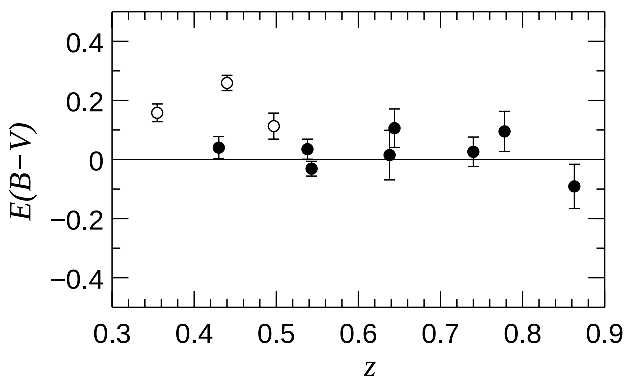

Fig. 4.— A plot of $E(B\text{-}V)$ as a function of redshift for the 11 HST-observed supernovae of this paper shows that the blue edge of the distribution shows no significant evolution with redshift. (The larger dispersion at lower redshifts is expected for a flux-limited sample.) Error bars include only measurement errors, and no assumed intrinsic color dispersion. Filled circles are those supernovae in the low-extinction subset (Subset 2).

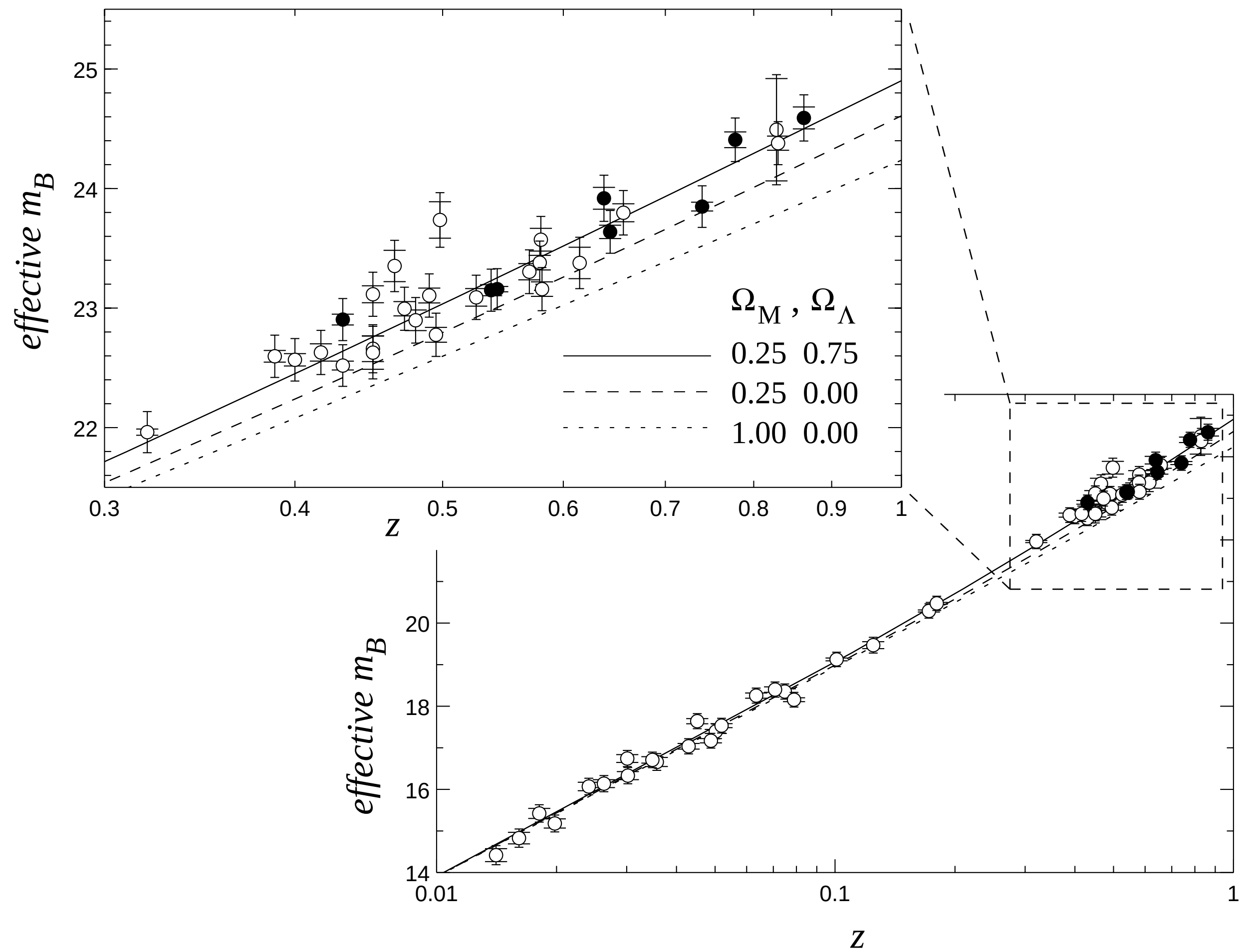

Fig. 5.— Hubble diagram of effective K- and stretch-corrected m_B vs. redshift for the supernovae in the primary low-extinction subset. Filled circles represent the HST supernovae of this paper. Inner error bars show just the measurement uncertainties; outer error bars include 0.17 magnitudes of intrinsic dispersion. The solid line is the best-fit flat-universe cosmology from the low-extinction subset; the dashed and dotted lines represent the indicated cosmologies.

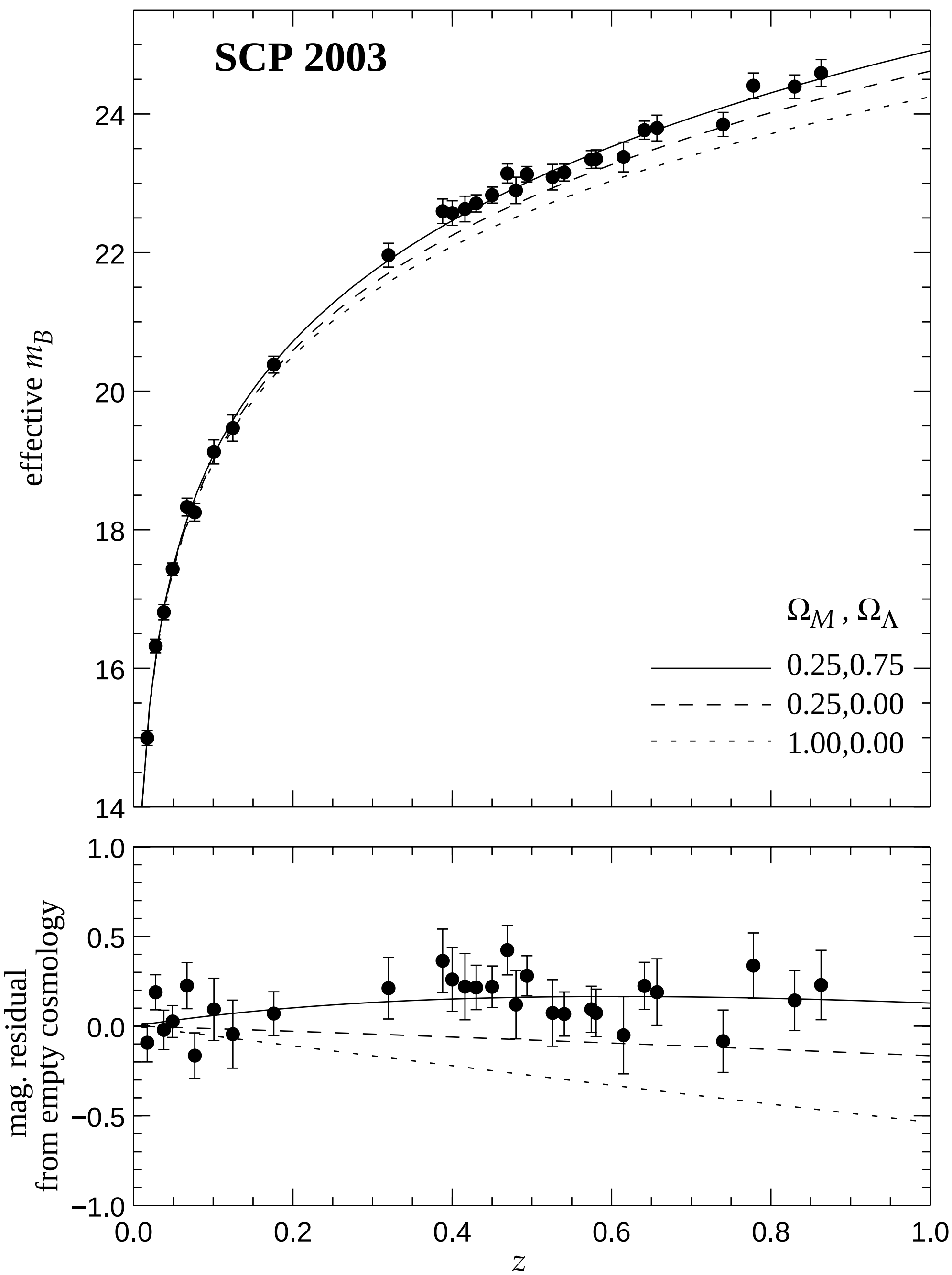

with a linear redshift scale

Fig. 6.— Upper panel: ~~Alternate~~ Hubble diagram, of effective m_B, with K-corrections, stretch corrections, and Galactic extinction corrections applied. For this plot, supernovae with redshifts within 0.01 of each other have been combined in a variance weighted sum. Only supernovae from the low-extinction subset are included. The solid line represents our best-fit flat-universe cosmology from the low-extinction subset; the dashed and dotted lines represent the indicated cosmologies. Lower panel: residuals of the data and lines in the upper panel from an empty universe ($\Omega_{\rm M} = 0$, $\Omega_\Lambda = 0$). As in the upper panel, supernovae with redshifts within 0.01 of each other have been combined.

[[[I think we should go with most of the caption modifications that Greg made, but with this one addition.]]]

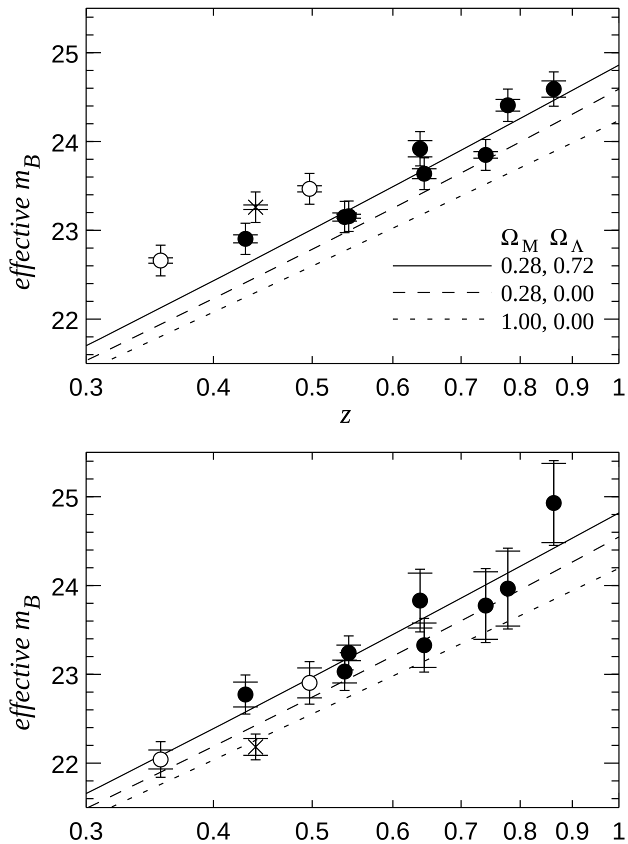

Fig. 7.— Hubble diagram of effective K- and stretch-corrected m_B vs. redshift for the 11 supernovae observed with WFPC2 and reported in this paper. Circles represent supernovae in the primary subset (Subset 1); the one point plotted as a cross (the very reddened supernova SN 1998aw) is omitted from that subset. Open circles represent reddened supernovae omitted from the low-extinction primary subset (Subset 2), while filled circles are in both Subsets 1 and 2. **Upper plot:** no host-galaxy $E(B\text{-}V)$ extinction corrections have been applied. Inner error bars only include the measurement error. Outer error bars include 0.17 magnitudes of intrinsic dispersion. **Lower plot:** extinction corrections have been applied using the standard interstellar extinction law. Error bars have been increased by the uncertainty in this extinction correction. Again, inner error bars represent only measurement uncertainties, while outer error bars include 0.11 magnitudes of intrinsic dispersion. Lines are for three example cosmologies with the indicated values of $\Omega_{\rm M}$ and Ω_Λ; the solid line is the best-fit flat-universe cosmology to our full primary subset with extinction corrections applied.

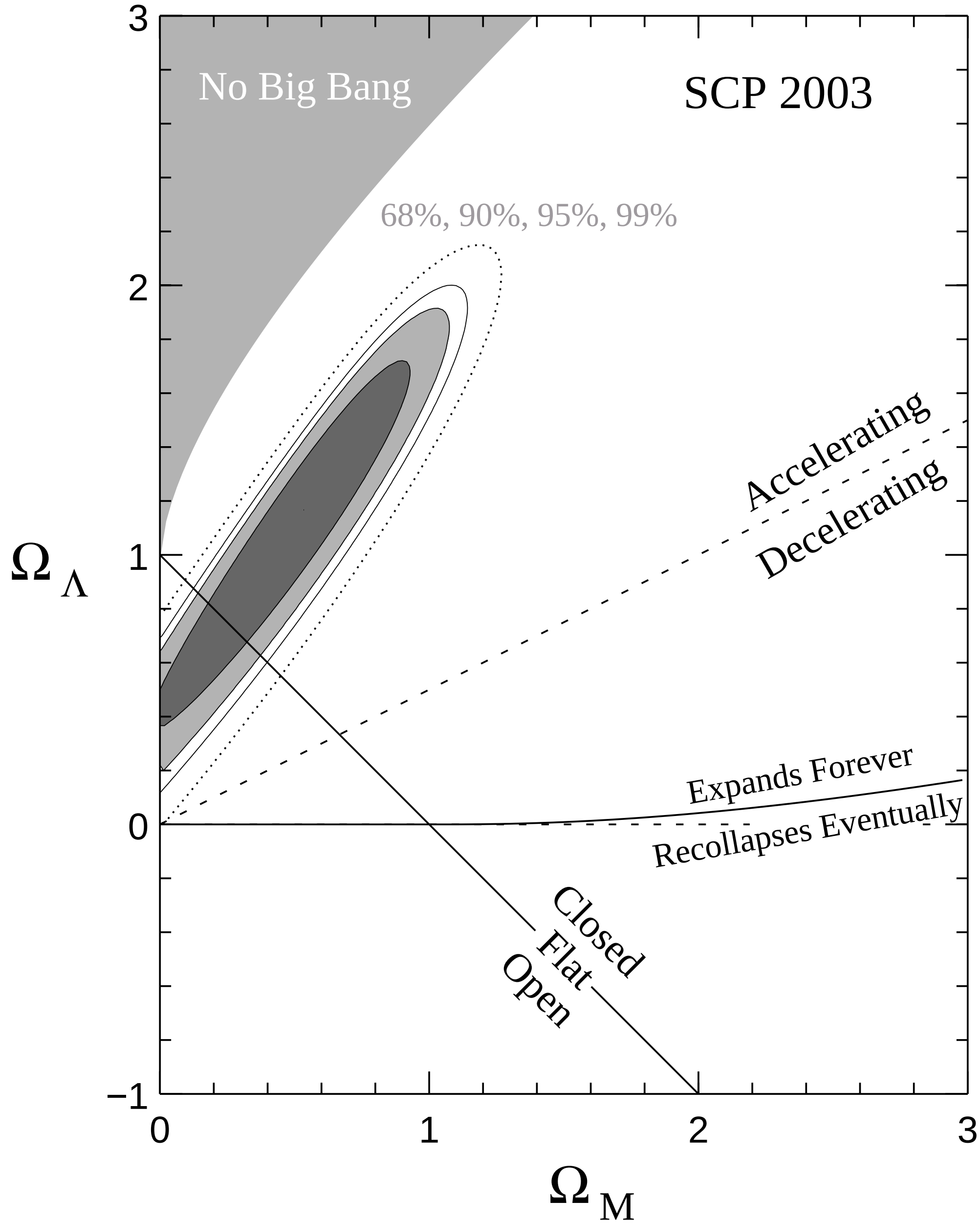

Fig. 8.— ~~Primary~~ 68%, 90%, 95%, and 99% confidence regions for Ω_{M} and Ω_Λ from ~~a~~ this paper's primary analysis, the fit to the low-extinction primary subset (Fit 3).

[[[Can you get a little more contract between these two shading colors?]]]

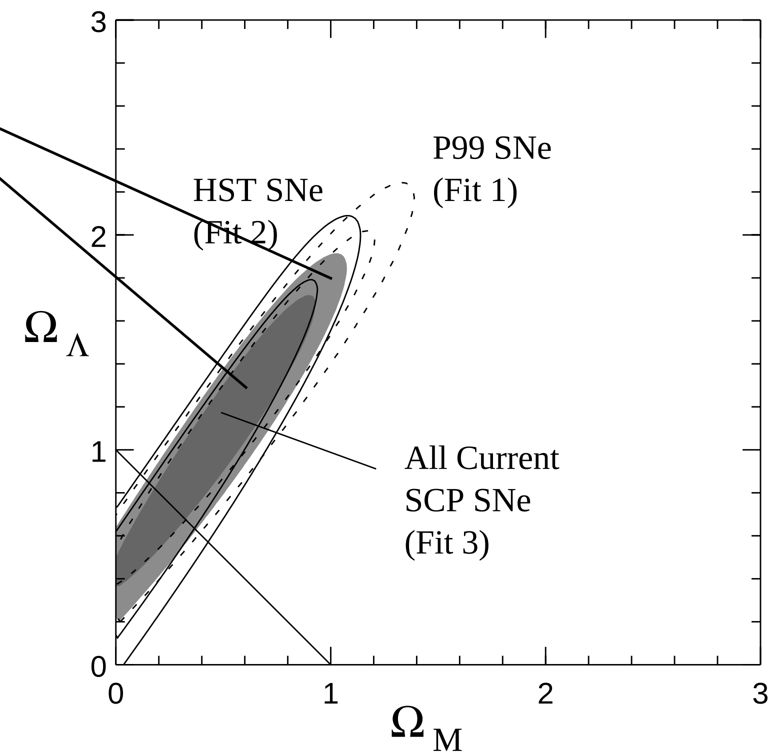

Fig. 9.— Contours indicate 68% and 90% confidence regions for fits to supernovae from the low-extinction primary subset, including just the high-redshift SNe from P99 (dotted lines), just the new HST high-redshift SNe (solid lines), and all SCP high-redshift SNe (filled contours). The low-redshift SNe from the primary subset are included in all fits. The new, independent sample of high-redshift supernovae provide measurements of Ω_M and Ω_Λ consistent with those from the P99 sample.

[[[Can "as Published" be centered under "Reiss et al. (1998)?]]]

[[[Also, make the words in this label lower-case, like they are in the following two labels, below.]]]

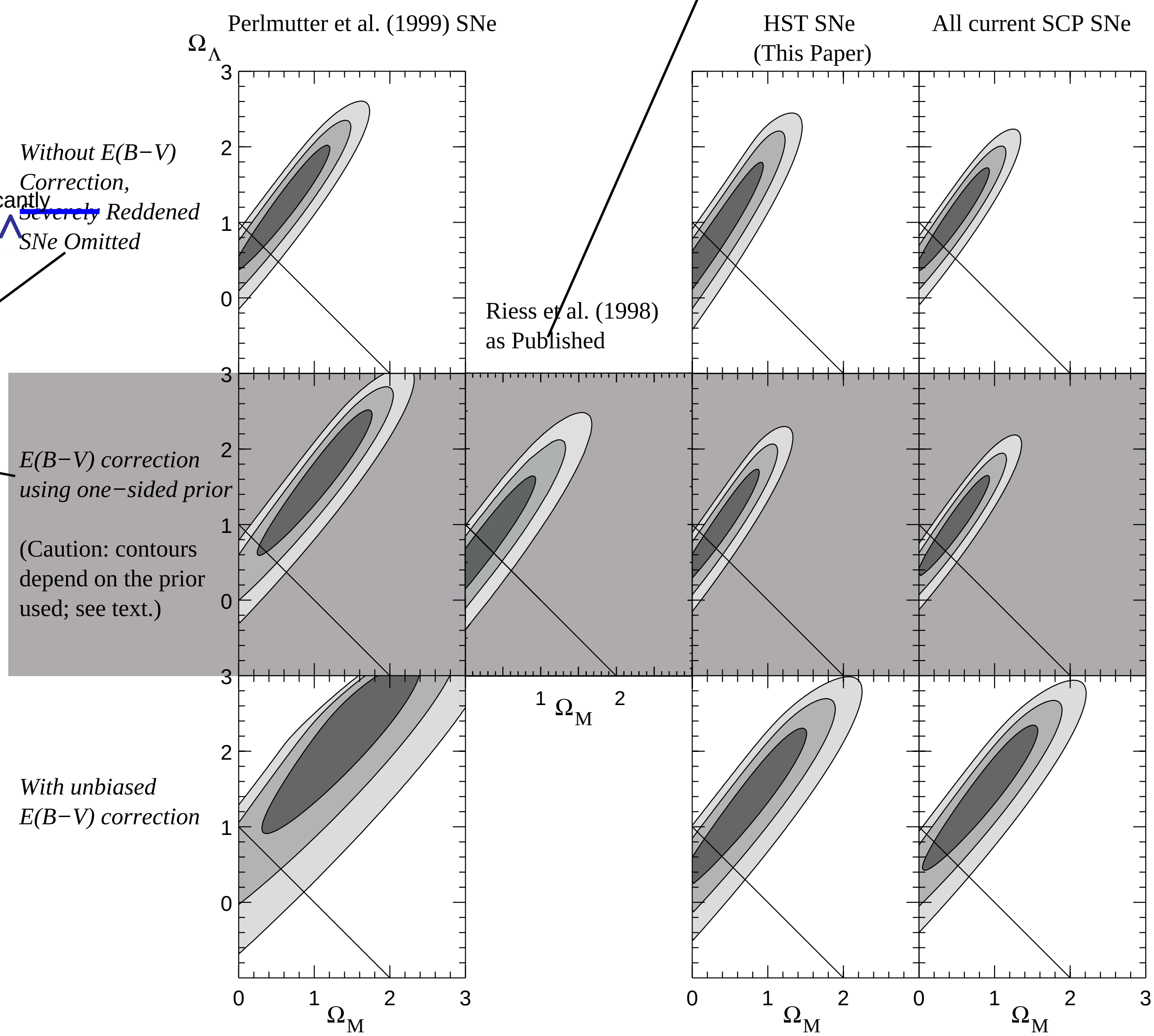

Fig. 10.— 68.3%, 95.4%, and 99.7% confidence regions for Ω_M and Ω_Λ using different data subsets and methods for treating host-galaxy extinction corrections. The top row represents our fits to the low-extinction primary subset, where significantly reddened supernovae have been omitted and host-galaxy extinction corrections are not applied. The second row shows fits where extinction corrections have been applied using a one-sided extinction prior. These fits are sensitive to the choice of prior, and can either yield results equivalent to analyses assuming low extinction (but without testing the assumption), or yield biased results (see text). Note that the published contours from Riess *et al.* (1998, their Fig. 6, solid contours) presented results from fits that included nine well-observed supernovae (that are comparable to the primary subsets used in the other panels), but also four supernovae with very sparsely sampled lightcurves, one supernova at $z = 0.97$ without a spectral confirmation, as well as two supernovae from the P99 set. The third row shows fits with unbiased extinction corrections applied to our primary subset. The HST SNe presented in this paper show a marked improvement in the precision of the color measurements, and hence in the precision of the Ω_M and Ω_Λ measurements when a full extinction correction is applied. With full and unbiased extinction corrections, dark energy is still required with $P(\Omega_\Lambda > 0) = 0.99$.

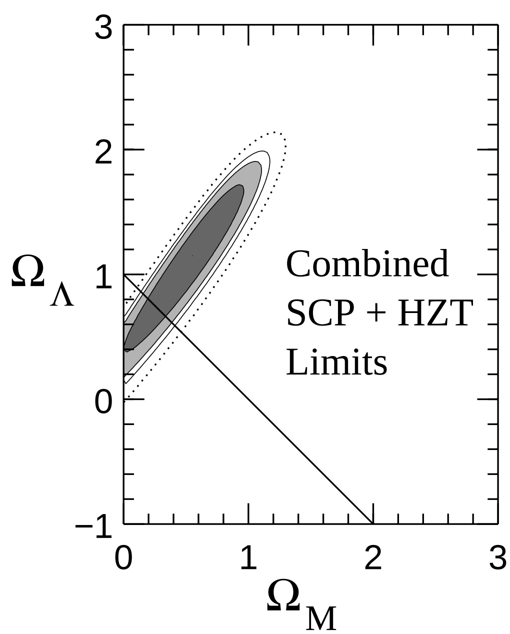

Fig. 11.— ~~Ω_M and Ω_Λ~~ 68%, 90%, 95%, and 99% confidence regions for Omega_M and Omega_Lambda, combining ~~which combine~~ the high-redshift data of the SCP (this paper and P99) and Riess *et al.* (1998). The fit includes Subset 2 supernovae from the SCP plus the nine well-observed confirmed SNe Ia from Riess *et al.* (1998).

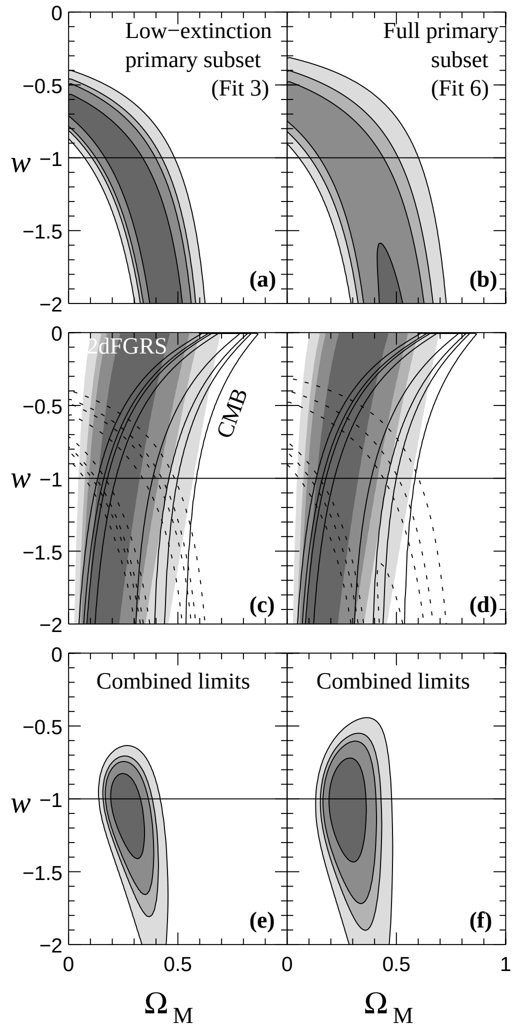

Fig. 12.— Joint measurements of Ω_M and w assuming $\Omega_M + \Omega_X = 1$ and that w is not time-varying. Confidence regions plotted are 68%, 90%, 95%, and 99%. The left column (panels a, c, and e) shows fits to the low-extinction primary subset; the right column (panels b, d, and f) shows fits to the primary subset with unbiased individual host-galaxy extinction corrections applied to each supernova. The upper panels (a and b) show the confidence intervals from the SCP supernovae alone. The middle panels (c and d) overlay this (dotted lines) with measurements from 2dFGRS (filled contours) (Hawkins *et al.* 2002) and combined CMB measurements (solid contours) (Bennett *et al.* 2003; Spergel *et al.* 2003). The bottom panels (e and f) combine the three confidence regions to provide a combined measurement of Ω_M and w.

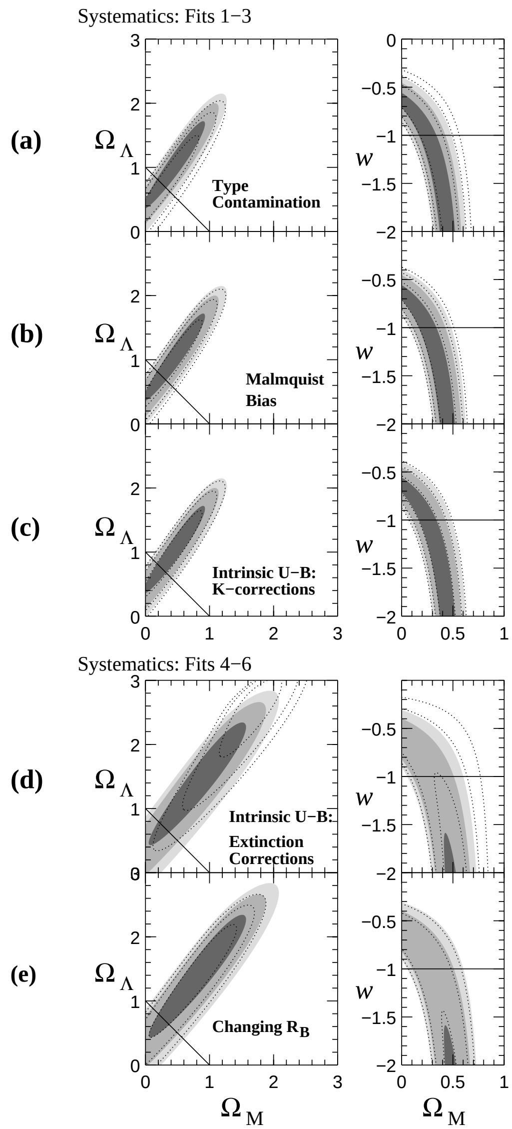

the fit to the full primary subset,

Fig. 13.— Simulated effects of identified systematic errors on the cosmological parameters, estimated by applying the systematic effect to the supernova parameters used in the cosmological fits. The left column shows fits to Ω_{M} and Ω_{Λ}, and the right column to Ω_{M} and the dark energy equation of state parameter w. Rows (a)–(c) show our primary fit (Fit 3) in filled contours. (a) The dotted contours show the results of a fit to Subset 3, only those supernovae with the most secure spectral identifications as Type Ia SNe. (b) The dotted contours show a fit to Subset 1 where the supernova magnitudes have been dimmed to correct for Malmquist bias. (c) The dotted contours show a fit to Subset 2, where K-corrections have been applied using a template spectrum with an intrinsic value of U-B= 0.5 at the epoch of B-maximum. (d) The filled contours is Fit 6, ~~our standard fit~~ with host-galaxy extinction corrections applied; the dotted contours show a fit to the same Subset, but using a template spectrum with an intrinsic value of U-B= 0.5 for estimating both K-corrections and color excesses. (e) The dotted contours apply extinction corrections to Subset 1 using a value of $R_B = 3.5$ rather than the standard $R_B = 4.1$ which was used for Fit 6 (filled contours).

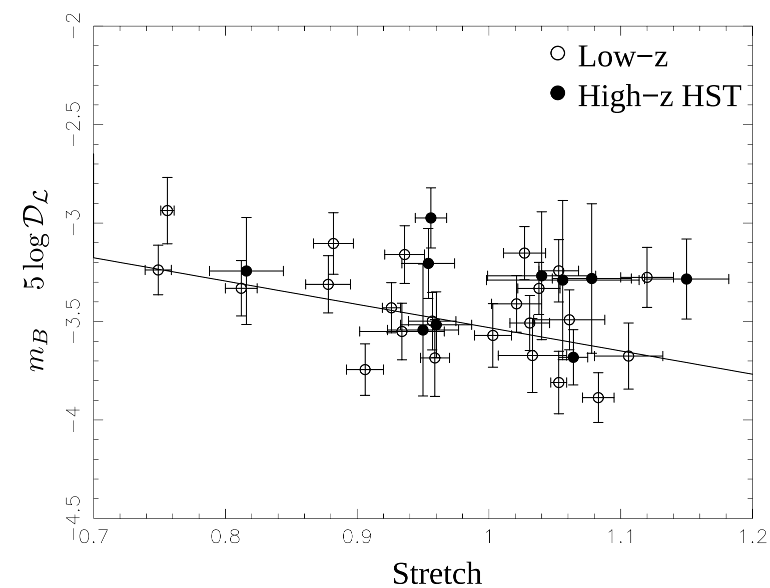

[[[Is this correct? Are these points extinction corrected?]]]

Fig. 14.— Stretch-luminosity relationship for low-redshift SNe (open circles) and high-redshift HST SNe (filled circles). Each point is the K-corrected and extinction-corrected m_B for that supernova, minus $\mathcal{D}_{\mathcal{L}}$, the "Hubble-constant-free luminosity distance" (see § 2.4), plotted against the stretch of that SN. The line drawn represents the best-fit values of α and $\mathcal{M}$ from Fit 6, the fit to all Subset 1 supernovae with host-galaxy extinction corrections applied. Note in particular that our HST SNe Ia all have low-redshift counterparts.

Table 1: WFPC2 Supernova Observations

SN Name	z	F675W Observations	F814W Observations
1997ek	0.863	1998-01-05 (400s,400s)	1998-01-05 (500s,700s)
		1998-01-11 (400s,400s)	1998-01-11 (500s,700s)
			1998-02-02 (1100s,1200s)
			1998-02-14 (1100s,1200s)
			1998-02-27 (1100s,1200s)
			1998-11-09 (1100s,1300s)
			1998-11-16 (1100s,1300s)
1997eq	0.538	1998-01-06 (300s,300s)	1998-01-06 (300s,300s)
		1998-01-21 (400s,400s)	1998-01-11 (300s,300s)
			1998-02-02 (500s,700s)
		1998-02-11 (400s,400s)	1998-02-11 (500s,700s)
		1998-02-19 (400s,400s)	1998-02-19 (500s,700s)
1997ez	0.778	1998-01-05 (400s,400s)	1998-01-05 (500s,700s)
		1998-01-11 (400s,400s)	1998-01-11 (500s,700s)
			1998-02-02 (1100s,1200s)
			1998-02-14 (1100s,1200s)
			1998-02-27 (100s,1200s,1100s,1200s)
1998as	0.355	1998-04-08 (400s,400s)	1998-04-08 (500s,700s)
		1998-04-20 (400s,400s)	1998-04-20 (500s,700s)
		1998-05-11 (400s,400s)	1998-05-11 (500s,700s)
		1998-05-15 (400s,400s)	1998-05-15 (500s,700s)
		1998-05-29 (400s,400s)	1998-05-29 (500s,700s)
1998aw	0.440	1998-04-08 (300s,300s)	1998-04-08 (300s,300s)
		1998-04-18 (300s,300s)	1998-04-18 (300s,300s)
		1998-04-29 (400s,400s)	1998-04-29 (500s,700s)
		1998-05-14 (400s,400s)	1998-05-14 (500s,700s)
		1998-05-28 (400s,400s)	1998-05-28 (500s,700s)
1998ax	0.497	1998-04-08 (300s,300s)	1998-04-08 (300s,300s)
		1998-04-18 (300s,300s)	1998-04-18 (300s,300s)
		1998-04-29 (300s,300s)	1998-04-29 (500s,700s)
		1998-05-14 (300s,300s)	1998-05-14 (500s,700s)
		1998-05-27 (300s,300s)	1998-05-27 (500s,700s)
1998ay	0.638	1998-04-08 (400s,400s)	1998-04-08 (500s,700s)
		1998-04-20 (400s,400s)	1998-04-20 (500s,700s)
			1998-05-11 (1100s,1200s)
			1998-05-15 (1100s,1200s)
			1998-06-03 (1100s,1200s)
1998ba	0.430	1998-04-08 (300s,300s)	1998-04-08 (300s,300s)
		1998-04-19 (300s,300s)	1998-04-19 (300s,300s)
		1998-04-29 (400s,400s)	1998-04-29 (500s,700s)
		1998-05-13 (400s,400s)	1998-05-13 (500s,700s)
		1998-05-28 (400s,400s)	1998-05-28 (500s,700s)
1998be	0.644	1998-04-08 (300s,300s)	1998-04-08 (300s,300s)
		1998-04-19 (300s,300s)	1998-04-19 (300s,300s)
		1998-04-30 (400s,400s)	1998-04-30 (500s,700s)
		1998-05-15 (400s,400s)	1998-05-15 (500s,700s)
		1998-05-28 (400s,400s)	1998-05-28 (500s,700s)
1998bi	0.740	1998-04-06 (400s,400s)	1998-04-06 (500s,700s)
		1998-04-18 (400s,400s)	1998-04-18 (500s,700s)
			1998-04-28 (1100s,1200s)
			1998-05-12 (1100s,1200s)
			1998-06-02 (1100s,1200s)
2000fr	0.543		2000-05-08 (2200s)
		2000-05-15 (600s,600s)	2000-05-15 (1100s,1100s)
		2000-05-28 (600s,600s)	2000-05-28 (600s,600s)
		2000-06-10 (500s,500s)	2000-06-10 (600s,600s)
		2000-06-22 (1100s,1300s)	2000-06-22 (1100s,1200s)
		2000-07-08 (1100s,1300s)	2000-07-08 (110s,1200s)

Table 2: U, V, and R Lightcurve Templates Used

Day[a]	U flux[b]	V flux[b]	R flux[b]	Day[1]	U flux[b]	V flux[b]	R flux[b]
-19	6.712e-03	4.960e-03	5.779e-03	31	4.790e-02	2.627e-01	3.437e-01
-18	2.685e-02	1.984e-02	2.312e-02	32	4.524e-02	2.481e-01	3.238e-01
-17	6.041e-02	4.464e-02	5.201e-02	33	4.300e-02	2.345e-01	3.054e-01
-16	1.074e-01	7.935e-02	9.246e-02	34	4.112e-02	2.218e-01	2.887e-01
-15	1.678e-01	1.240e-01	1.445e-01	35	3.956e-02	2.099e-01	2.733e-01
-14	2.416e-01	1.785e-01	2.080e-01	36	3.827e-02	1.990e-01	2.592e-01
-13	3.289e-01	2.430e-01	2.832e-01	37	3.722e-02	1.891e-01	2.463e-01
-12	4.296e-01	3.174e-01	3.698e-01	38	3.636e-02	1.802e-01	2.345e-01
-11	5.437e-01	4.017e-01	4.681e-01	39	3.565e-02	1.721e-01	2.237e-01
-10	6.712e-01	4.960e-01	5.779e-01	40	3.506e-02	1.649e-01	2.137e-01
-9	7.486e-01	5.889e-01	6.500e-01	41	3.456e-02	1.583e-01	2.046e-01
-8	8.151e-01	6.726e-01	7.148e-01	42	3.410e-02	1.524e-01	1.962e-01
-7	8.711e-01	7.469e-01	7.725e-01	43	3.365e-02	1.471e-01	1.884e-01
-6	9.168e-01	8.115e-01	8.236e-01	44	3.318e-02	1.423e-01	1.813e-01
-5	9.524e-01	8.660e-01	8.681e-01	45	3.266e-02	1.378e-01	1.747e-01
-4	9.781e-01	9.103e-01	9.062e-01	46	3.205e-02	1.337e-01	1.687e-01
-3	9.940e-01	9.449e-01	9.382e-01	47	3.139e-02	1.299e-01	1.630e-01
-2	1.000e+00	9.706e-01	9.639e-01	48	3.072e-02	1.263e-01	1.578e-01
-1	9.960e-01	9.880e-01	9.834e-01	49	3.005e-02	1.229e-01	1.529e-01
0	9.817e-01	9.976e-01	9.957e-01	50	2.945e-02	1.195e-01	1.483e-01
1	9.569e-01	1.000e+00	1.000e+00	51	2.893e-02	1.161e-01	1.440e-01
2	9.213e-01	9.958e-01	9.952e-01	52	2.853e-02	1.128e-01	1.398e-01
3	8.742e-01	9.856e-01	9.803e-01	53	2.830e-02	1.096e-01	1.359e-01
4	8.172e-01	9.702e-01	9.545e-01	54	2.827e-02	1.064e-01	1.320e-01
5	7.575e-01	9.502e-01	9.196e-01	55	2.849e-02	1.033e-01	1.282e-01
6	6.974e-01	9.263e-01	8.778e-01	56	2.793e-02	1.003e-01	1.244e-01
7	6.375e-01	8.991e-01	8.313e-01	57	2.738e-02	9.743e-02	1.207e-01
8	5.783e-01	8.691e-01	7.821e-01	58	2.684e-02	9.467e-02	1.170e-01
9	5.205e-01	8.369e-01	7.324e-01	59	2.630e-02	9.207e-02	1.133e-01
10	4.646e-01	8.031e-01	6.842e-01	60	2.578e-02	8.964e-02	1.097e-01
11	4.113e-01	7.683e-01	6.396e-01	61	2.527e-02	8.741e-02	1.061e-01
12	3.610e-01	7.330e-01	6.007e-01	62	2.477e-02	8.538e-02	1.026e-01
13	3.145e-01	6.977e-01	5.691e-01	63	2.428e-02	8.359e-02	9.910e-02
14	2.725e-01	6.629e-01	5.444e-01	64	2.380e-02	8.207e-02	9.568e-02
15	2.356e-01	6.293e-01	5.254e-01	65	2.333e-02	8.083e-02	9.232e-02
16	2.044e-01	5.972e-01	5.113e-01	66	2.287e-02	7.927e-02	8.902e-02
17	1.783e-01	5.667e-01	5.011e-01	67	2.242e-02	7.774e-02	8.579e-02
18	1.567e-01	5.376e-01	4.938e-01	68	2.197e-02	7.624e-02	8.264e-02
19	1.388e-01	5.099e-01	4.887e-01	69	2.154e-02	7.476e-02	7.958e-02
20	1.239e-01	4.835e-01	4.848e-01	70	2.111e-02	7.332e-02	7.660e-02
21	1.115e-01	4.583e-01	4.814e-01	71	2.070e-02	7.191e-02	7.373e-02
22	1.008e-01	4.342e-01	4.776e-01	72	2.029e-02	7.052e-02	7.096e-02
23	9.144e-02	4.113e-01	4.725e-01	73	1.989e-02	6.916e-02	6.832e-02
24	8.314e-02	3.894e-01	4.653e-01	74	1.949e-02	6.782e-02	6.581e-02
25	7.583e-02	3.685e-01	4.552e-01	75	1.911e-02	6.651e-02	6.344e-02
26	6.941e-02	3.486e-01	4.414e-01	76	1.873e-02	6.523e-02	6.199e-02
27	6.380e-02	3.296e-01	4.247e-01	77	1.836e-02	6.397e-02	6.057e-02
28	5.891e-02	3.115e-01	4.058e-01	78	1.799e-02	6.274e-02	5.918e-02
29	5.467e-02	2.943e-01	3.855e-01	79	1.764e-02	6.153e-02	5.783e-02
30	5.102e-02	2.781e-01	3.645e-01	80	1.729e-02	6.034e-02	5.650e-02

a: Day is relative to the epoch of the maximum of the B-band lightcurve. The B-band template may be found in Goldhaber *et al.* (2001).

b: Relative fluxes.

[[[The footnote c would be much better written using an equation (like this one, based on the footnote 9 of Table 1 of P99). Is this equation correct here?]]]

Stretch luminosity corrected effective B-band peak magnitude: {m_B}^{eff} \equiv m_X + \alpha(s -1) - K_{BX} - A_X .

Table 3: Supernova Lightcurve Fits: HST Supernovae from this paper

SN	z	m_X[a]	m_B[b]	m_{Beff}[c]	m_{Beff}[d]	Stretch	R-I[e]	$E(B$-$V)$ Gal.[f]	$E(B$-$V)^g_{\rm host}$	Exclud Subsets
1997ek	0.863	23.32	24.51 ± 0.03	24.59 ± 0.19	24.95 ± 0.44	1.056 ± 0.058	0.838 ± 0.054	0.042	0.091 ± 0.075	
1997eq	0.538	22.63	23.21 ± 0.02	23.15 ± 0.18	23.02 ± 0.17	0.960 ± 0.027	0.202 ± 0.030	0.044	0.035 ± 0.034	
1997ez	0.778	23.17	24.29 ± 0.03	24.41 ± 0.18	24.00 ± 0.42	1.078 ± 0.030	0.701 ± 0.048	0.026	0.095 ± 0.068	
1998as	0.355	22.18	22.72 ± 0.03	22.66 ± 0.17	22.02 ± 0.15	0.956 ± 0.012	0.226 ± 0.027	0.037	0.158 ± 0.030	2,3
1998aw	0.440	22.56	23.22 ± 0.02	23.26 ± 0.17	22.19 ± 0.15	1.026 ± 0.019	0.300 ± 0.024	0.026	0.259 ± 0.026	1–3
1998ax	0.497	22.63	23.25 ± 0.05	23.47 ± 0.17	22.96 ± 0.20	1.150 ± 0.032	0.212 ± 0.041	0.035	0.113 ± 0.044	2,3
1998ay	0.638	23.26	23.86 ± 0.08	23.92 ± 0.19	23.85 ± 0.33	1.040 ± 0.041	0.339 ± 0.067	0.035	0.015 ± 0.084	3
1998ba	0.430	22.34	22.97 ± 0.05	22.90 ± 0.18	22.75 ± 0.18	0.954 ± 0.020	0.094 ± 0.036	0.024	0.040 ± 0.038	
1998be	0.644	23.33	23.91 ± 0.04	23.64 ± 0.18	23.26 ± 0.27	0.816 ± 0.028	0.436 ± 0.051	0.029	0.106 ± 0.065	3
1998bi	0.740	22.86	23.92 ± 0.02	23.85 ± 0.17	23.75 ± 0.37	0.950 ± 0.027	0.552 ± 0.037	0.026	0.026 ± 0.050	
2000fr	0.543	22.44	23.07 ± 0.02	23.16 ± 0.17	23.27 ± 0.14	1.064 ± 0.011	0.135 ± 0.022	0.030	0.031 ± 0.025	

a: Magnitude in the observed filter at the peak of the rest-frame B-band lightcurve. X=R for $z < 0.7$, X=I for $z > 0.7$.

b: This value has been K-corrected and corrected for Galactic extinction. These were the values used in the cosmological fits.

c: This is ~~the value in column b, including the stretch correction~~ using the best-fit value of the stretch/luminosity slope from the fit to the primary low-extinction subset (Fit!3 in § 4). The uncertainty includes all uncertainties for non-extinction corrected fits described in § 2.4. Note that these values are only provided for convenience; ~~due to the fact that the stretch/luminosity slope is a fit parameter,~~ they were not used directly in any cosmological fits.

since the slope, alpha, of the stretch-luminosity relation is also a fit parameter.

d: Similar to column c, only with the host-galaxy extinction correction applied. The stretch/luminosity slope used for this value is that from the fit to the primary subset (Fit 6 in § 4). Uncertainties include all uncertainties for extinction-corrected fits described in § 2.4.

e: This is the observed R-I color at the epoch of the rest-frame B-band lightcurve peak.

f: Schlegel, Finkbeiner, & Davis (1998); this extinction is already included in the quoted values of m_B.

g: Measurement uncertainty only; no intrinsic color dispersion included.

h: These supernovae are excluded from the indicated subsets; see § 2.5.

Table 4: Supernova Lightcurve Fits: New Fits to Perlmutter (1999) SNe

SN	z	${m_X}^a$	${m_B}^b$	${m_{Beff}}^c$	${m_{Beff}}^d$	Stretch	R-I^e	$E(B$-$V)$ Gal.^{f}	$E(B$-$V)^g_{\rm host}$	Excluc Subset
1995ar	0.465	22.80	23.48 ± 0.08	23.35 ± 0.22	21.54 ± 0.97	0.909 ± 0.104	0.509 ± 0.222	0.022	0.448 ± 0.242	
1995as	0.498	23.03	23.69 ± 0.07	23.74 ± 0.23	23.52 ± 0.87	1.035 ± 0.090	0.155 ± 0.197	0.021	0.051 ± 0.212	3
1995aw	0.400	21.78	22.28 ± 0.03	22.57 ± 0.18	23.17 ± 0.45	1.194 ± 0.037	0.127 ± 0.103	0.040	0.160 ± 0.107	
1995ax	0.615	22.56	23.21 ± 0.06	23.38 ± 0.22	23.98 ± 1.02	1.112 ± 0.073	0.152 ± 0.204	0.033	0.153 ± 0.249	
1995ay	0.480	22.64	23.07 ± 0.04	22.90 ± 0.19	22.74 ± 0.70	0.880 ± 0.064	0.209 ± 0.158	0.114	0.047 ± 0.170	
1995az	0.450	22.46	22.70 ± 0.07	22.66 ± 0.20	23.04 ± 0.58	0.973 ± 0.064	0.087 ± 0.135	0.181	0.089 ± 0.144	
1995ba	0.388	22.07	22.64 ± 0.06	22.60 ± 0.18	22.74 ± 0.45	0.971 ± 0.047	0.006 ± 0.105	0.018	0.033 ± 0.110	
1996cf	0.570	22.71	23.31 ± 0.03	23.30 ± 0.18	23.53 ± 0.45	0.996 ± 0.045	0.162 ± 0.091	0.040	0.054 ± 0.107	3
1996cg	0.490	22.46	23.09 ± 0.03	23.11 ± 0.18	22.26 ± 0.45	1.011 ± 0.040	0.300 ± 0.099	0.035	0.205 ± 0.107	3
1996ci	0.495	22.19	22.83 ± 0.02	22.78 ± 0.18	22.92 ± 0.32	0.964 ± 0.040	0.083 ± 0.070	0.028	0.033 ± 0.075	
1996cl	0.828	23.37	24.53 ± 0.17	24.49 ± 0.46	25.92 ± 0.97	0.974 ± 0.239	0.549 ± 0.184	0.035	0.344 ± 0.251	
1996cm	0.450	22.67	23.26 ± 0.07	23.11 ± 0.18	22.63 ± 0.77	0.899 ± 0.061	0.214 ± 0.174	0.049	0.124 ± 0.185	3
1996cn	0.430	22.58	23.25 ± 0.03	23.09 ± 0.19	21.76 ± 0.41	0.890 ± 0.066	0.379 ± 0.090	0.025	0.332 ± 0.097	1–3
1997F	0.580	22.93	23.51 ± 0.06	23.57 ± 0.20	23.30 ± 0.95	1.041 ± 0.066	0.275 ± 0.197	0.040	0.063 ± 0.232	
1997H	0.526	22.70	23.26 ± 0.04	23.09 ± 0.19	22.51 ± 0.80	0.882 ± 0.043	0.303 ± 0.174	0.051	0.150 ± 0.194	
1997I	0.172	20.18	20.34 ± 0.01	20.29 ± 0.17	20.19 ± 0.28	0.967 ± 0.009	0.065 ± 0.047	0.051	0.026 ± 0.064	
1997N	0.180	20.39	20.38 ± 0.02	20.48 ± 0.17	21.28 ± 0.52	1.067 ± 0.015	0.141 ± 0.093	0.031	0.200 ± 0.123	
1997O	0.374	22.99	23.53 ± 0.06	23.60 ± 0.18	23.38 ± 0.66	1.048 ± 0.054	0.087 ± 0.152	0.029	0.049 ± 0.162	1–3
1997P	0.472	22.53	23.16 ± 0.04	22.99 ± 0.18	23.24 ± 0.91	0.888 ± 0.039	0.058 ± 0.207	0.033	0.052 ± 0.219	
1997Q	0.430	22.01	22.61 ± 0.02	22.52 ± 0.17	22.55 ± 0.62	0.935 ± 0.024	0.061 ± 0.140	0.030	0.002 ± 0.148	
1997R	0.657	23.29	23.89 ± 0.05	23.80 ± 0.19	23.68 ± 0.90	0.940 ± 0.059	0.393 ± 0.175	0.030	0.032 ± 0.222	
1997ac	0.320	21.42	21.87 ± 0.02	21.96 ± 0.17	21.95 ± 0.33	1.061 ± 0.015	0.063 ± 0.065	0.027	0.001 ± 0.072	
1997af	0.579	22.94	23.60 ± 0.07	23.38 ± 0.18	24.31 ± 1.09	0.850 ± 0.045	0.045 ± 0.226	0.028	0.215 ± 0.265	
1997ai	0.450	22.34	22.94 ± 0.05	22.63 ± 0.22	22.58 ± 0.59	0.788 ± 0.084	0.143 ± 0.133	0.045	0.026 ± 0.142	
1997aj	0.581	22.58	23.24 ± 0.07	23.16 ± 0.18	24.05 ± 0.79	0.947 ± 0.045	0.045 ± 0.164	0.033	0.213 ± 0.193	
1997am	0.416	22.01	22.58 ± 0.08	22.63 ± 0.18	22.65 ± 0.46	1.032 ± 0.060	0.037 ± 0.113	0.036	0.008 ± 0.119	
1997ap	0.830	23.16	24.35 ± 0.07	24.38 ± 0.18	23.74 ± 0.50	1.023 ± 0.045	0.903 ± 0.082	0.026	0.155 ± 0.118	

a: X=R for $z < 0.7$, X=I for $z > 0.7$

b: This value has been K-corrected and corrected for Galactic extinction.

[[[It's probably better to just copy the same footnote as in the other tables, here -- just like all the other footnotes -- instead of referring to the other table.]]]

c: Includes the stretch/luminosity correction and all uncertainties used in fits to the low-extinction subset; see note *c* in Table 3.

d: Includes the stretch/luminosity and host-galaxy extinction corrections, and all uncertainties used in fits with host-galaxy extinction corrections applied; see note *d* in Table 3.

e: This is the observed R-I color at the epoch of the rest-frame B-band lightcurve peak.

f: Schlegel, Finkbeiner, & Davis (1998); this extinction is already included in the quoted values of m_B.

g: Measurement uncertainty only; no intrinsic color dispersion included.

h: These supernovae are excluded from the indicated subsets; see § 2.5.

I think this column should not be m_X, but rather m_B^observed (and then the next column should be m_B with a superscript referring to a footnote that says it is the m_B^observed - K_{BB} where K_{BB} is the B band K correction).

Footnote superscript "a" should now be moved over here, to column 1, i.e., SN^a

Table 5: Supernova Lightcurve Fits: Low-z SNe from Hamuy (1996) and Riess (1999)

SN	z	m_X[a]	m_B[b]	m_{Beff}[c]	m_{Beff}[d]	Stretch	R-I[e]	$E(B-V)$ Gal.[f]	$E(B-V)^{g}_{\rm host}$	Exclud Subsets
1990O	0.030	16.58	16.18 ± 0.03	16.33 ± 0.20	16.30 ± 0.17	1.106 ± 0.026	0.043 ± 0.025	0.098	0.001 ± 0.026	
1990af	0.050	17.92	17.76 ± 0.01	17.39 ± 0.18	17.42 ± 0.13	0.749 ± 0.010	0.077 ± 0.011	0.035	0.011 ± 0.011	
1992P	0.026	16.12	16.05 ± 0.02	16.14 ± 0.19	16.16 ± 0.16	1.061 ± 0.027	0.045 ± 0.018	0.020	0.008 ± 0.019	
1992ae	0.075	18.59	18.42 ± 0.04	18.35 ± 0.18	18.35 ± 0.15	0.957 ± 0.018	0.098 ± 0.028	0.036	0.003 ± 0.031	
1992ag	0.026	16.67	16.26 ± 0.02	16.34 ± 0.20	15.55 ± 0.16	1.053 ± 0.015	0.220 ± 0.020	0.097	0.189 ± 0.021	2,3
1992al	0.014	14.61	14.48 ± 0.01	14.42 ± 0.23	14.53 ± 0.20	0.959 ± 0.011	0.054 ± 0.012	0.034	0.025 ± 0.013	
1992aq	0.101	19.38	19.30 ± 0.02	19.12 ± 0.17	19.24 ± 0.15	0.878 ± 0.017	0.142 ± 0.023	0.012	0.019 ± 0.026	
1992bc	0.020	15.18	15.10 ± 0.01	15.18 ± 0.20	15.36 ± 0.16	1.053 ± 0.006	0.087 ± 0.009	0.022	0.046 ± 0.009	
1992bg	0.036	17.41	16.66 ± 0.04	16.66 ± 0.20	16.68 ± 0.16	1.003 ± 0.014	0.128 ± 0.025	0.181	0.006 ± 0.026	
1992bh	0.045	17.71	17.60 ± 0.02	17.64 ± 0.18	17.22 ± 0.14	1.027 ± 0.016	0.101 ± 0.018	0.022	0.100 ± 0.019	
1992bl	0.043	17.37	17.31 ± 0.03	17.03 ± 0.18	17.10 ± 0.14	0.812 ± 0.012	0.017 ± 0.023	0.012	0.002 ± 0.024	
1992bo	0.018	15.89	15.78 ± 0.01	15.42 ± 0.21	15.31 ± 0.17	0.756 ± 0.005	0.048 ± 0.012	0.027	0.043 ± 0.012	
1992bp	0.079	18.59	18.29 ± 0.01	18.16 ± 0.18	18.41 ± 0.13	0.906 ± 0.014	0.088 ± 0.015	0.068	0.056 ± 0.017	
1992br	0.088	19.52	19.37 ± 0.08	18.93 ± 0.20	18.89 ± 0.19	0.700 ± 0.021	0.186 ± 0.047	0.027	0.030 ± 0.052	1–3
1992bs	0.063	18.26	18.20 ± 0.04	18.26 ± 0.18	18.37 ± 0.14	1.038 ± 0.016	0.011 ± 0.022	0.013	0.031 ± 0.024	
1993B	0.071	18.74	18.37 ± 0.04	18.40 ± 0.18	18.10 ± 0.15	1.021 ± 0.019	0.181 ± 0.027	0.080	0.071 ± 0.029	
1993O	0.052	17.87	17.64 ± 0.01	17.53 ± 0.18	17.61 ± 0.13	0.926 ± 0.007	0.042 ± 0.012	0.053	0.014 ± 0.012	
1993ag	0.050	18.32	17.83 ± 0.02	17.73 ± 0.18	17.26 ± 0.15	0.936 ± 0.015	0.217 ± 0.020	0.111	0.120 ± 0.021	2,3
1994M	0.024	16.34	16.24 ± 0.03	16.07 ± 0.20	15.84 ± 0.16	0.882 ± 0.015	0.043 ± 0.022	0.023	0.063 ± 0.022	
1994S	0.016	14.85	14.78 ± 0.02	14.83 ± 0.22	14.86 ± 0.19	1.033 ± 0.026	0.061 ± 0.019	0.018	0.010 ± 0.019	
1995ac	0.049	17.23	17.05 ± 0.01	17.17 ± 0.18	17.17 ± 0.13	1.083 ± 0.012	0.026 ± 0.011	0.042	0.005 ± 0.011	
1995bd	0.016	17.34	15.32 ± 0.01	15.37 ± 0.30	13.94 ± 0.27	1.039 ± 0.008	0.735 ± 0.008	0.490	0.348 ± 0.009	1–3
1996C	0.030	16.62	16.57 ± 0.04	16.74 ± 0.19	16.50 ± 0.16	1.120 ± 0.020	0.012 ± 0.026	0.014	0.051 ± 0.027	
1996ab	0.125	19.72	19.57 ± 0.04	19.47 ± 0.19	19.82 ± 0.16	0.934 ± 0.032	0.174 ± 0.025	0.032	0.082 ± 0.029	
1996bl	0.035	17.08	16.66 ± 0.01	16.71 ± 0.19	16.55 ± 0.14	1.031 ± 0.015	0.093 ± 0.012	0.099	0.036 ± 0.012	
1996bo	0.016	16.18	15.85 ± 0.01	15.65 ± 0.22	14.12 ± 0.18	0.862 ± 0.006	0.406 ± 0.008	0.077	0.383 ± 0.008	1–3

a: Supernovae through 1993ag are from H96, later ones from R99.

b: This is the measured peak magnitude of the *B*-band lightcurve.

[[Copy full footnote here too.]]

c: Includes the stretch/luminosity correction and all uncertainties used in fits to the low-extinction subset; see note *c* in Table 3.

d: Includes the stretch/luminosity and host-galaxy extinction corrections, and all uncertainties used in fits with host-galaxy extinction corrections applied; see note *d* in Table 3.

e: This value has been *K*-corrected and corrected for Galactic extinction.

f: This is the measured *B*-*V* color at the epoch of rest-frame *B*-band lightcurve maximum.

g: Schlegel, Finkbeiner, & Davis (1998); this extinction is already included in the quoted values of m_B in column *c*.

h: These supernovae are excluded from the indicated subsets; § 2.5.

[[[I think almost all of these footnotes (or the superscripts connected to them) are incorrect -- they don't refer to the correct columns.]]]

Table 6: U-B SN Ia Colors at Epoch of B-band Maximum

SN	Raw U-B^a	Corrected U-B^b	Reference
1980N	0.21	0.29	Hamuy *et al.* (1991)
1989B	0.08	0.33	Wells *et al.* (1994)
1990N	0.35	0.45	Lira *et al.* (1998)
1994D	0.50	0.52	Wu, Yan, & Zou (1995)
1998bu	0.23	0.51	Suntzeff *et al.* (1999)

a: This is the measured U-B value from the cited paper.

b: This U-B value is K-corrected, and corrected for host-galaxy and Galactic extinction.

Table 7: Mean $E(B$-$V)$ Values

Sample	Complete Set	Low-extinction Primary Subset SNe^a
Low z	$+0.095 \pm 0.003$	0.001 ± 0.003
P99	$+0.018 \pm 0.024$	0.004 ± 0.025
HST	$+0.090 \pm 0.012$	$+0.012 \pm 0.015$

a: SNe omitted from our low-extinction primary subset, Subset 2, (§ 2.5) have been omitted from these means. This excludes outliers, as well as supernovae with both $E(B$-$V) > 0.1$ and $E(B$-$V) > 2\sigma$ above zero.

Table 8: Cosmological fits

Fit #	High-Redshift SNe Included in Fit[a]	N_{SNe}	Min. χ^2	Ω_M for Flat[b]	Ω_Λ for Flat[b]	$P(\Omega_\Lambda > 0)$	$\mathcal{M}$	α
Fits to the Low-Extinction Primary Subset								
1	SNe from P99	46	52	$0.25^{+0.08}_{0.07}$	$0.75^{+0.07}_{0.07}$	0.9995	3.49 ± 0.05	1.58 ± 0.31
2	New HST SNe from this paper	29	30	$0.25^{+0.09}_{0.08}$	$0.75^{+0.08}_{0.09}$	0.9947	3.47 ± 0.05	1.06 ± 0.37
3	**All SCP SNe**	**54**	**60**	$\mathbf{0.25^{+0.07}_{0.06}}$	$\mathbf{0.75^{+0.06}_{0.07}}$	**0.9997**	$\mathbf{3.48 \pm 0.05}$	$\mathbf{1.47 \pm 0.29}$
Fits to Full Primary Subset, with Extinction Correction								
4	SNe from P99	48	56	$0.21^{+0.18}_{0.15}$	$0.79^{+0.15}_{0.18}$	0.9967	3.55 ± 0.05	1.30±0.30
5	New HST SNe from this paper	33	39	$0.27^{+0.12}_{0.10}$	$0.73^{+0.10}_{0.12}$	0.9953	3.54 ± 0.05	1.29±0.28
6	All SCP SNe	58	65	$0.28^{+0.11}_{0.10}$	$0.72^{+0.10}_{0.11}$	0.9974	3.53 ± 0.05	1.18±0.30

a: All fits include the low-redshift SNe from H96 and R99. See § 2.5 for the definitions of the supernova subsets.
b: This is the intersection of the fit probability distribution with the line $\Omega_M + \Omega_\Lambda = 1$.

Uncertainties
Table 9: Identified Systematic ~~Errors~~

Source of Uncertainty	Systematic Uncertainty On: Flat-Universe Ω_M or Ω_Λ [a]	$\Omega_M + \Omega_\Lambda$	constant w [b]	Notes
Fit method	0.03 (0.5σ)	0.80	0.02	
Type contamination	0.03 (0.5σ)	0.48	0.07	
Malmquist Bias	0.01 (0.2σ)	0.18	0.03	
Intrinsic U-B: K-corrections	0.00 (0.0σ)	0.13	0.01	c
Gravitational Lensing	0.01 (0.2σ)	0.04	0.05	
Systematic with host-galaxy extinction corrections:				
Intrinsic U-B: color excess	0.07 (0.7σ)	1.78	0.10	d
Extinction Slope	0.00 (0.0σ)	0.18	0.01	d
Dust Evolution	0.03 (0.3σ)	0.02	0.06	d

a: Each systematic is given as an offset from the flat-universe value of Ω_M, and in terms of the smaller side of the statistical error bar (0.06 for Fit 3 to the low-extinction subset, 0.10 for Fit 6 to the full primary subset).

b: This is the offset on the maximum-likelihood value of w when the fit ~~the low-extinction subset fits (Fit 3)~~ is combined with the 2dFGRS and CMB measurements.

c: Only used where host-galaxy extinction corrections are not applied.

d: Only used where host-galaxy extinction corrections are applied.